GeoArabia, 2012, v. 17, no. 2, p. 155-184
Gulf PetroLink, Bahrain

Biostratigraphy and carbon-isotope stratigraphy of the uppermost Aptian to Upper Cenomanian strata of the South Palmyrides, Syria

Hussam Ghanem, Mikhail Mouty and Jochen Kuss

ABSTRACT

Biostratigraphic and carbon-isotope data were used to introduce a high-resolution stratigraphic reference section of the Upper Aptian to Upper Cenomanian platform carbonates of the South Palmyrides in Syria. We studied the biostratigraphic evolution of the Zbeideh to Abou-Zounnar formations in two sections, based on 42 species of benthonic foraminifera and 38 species of planktonic foraminifera. Comparisons with other Tethyan assemblages allowed determining 11 biozones; six are based on planktonic foraminifera, and five on benthonic foraminifera. Four hiatuses (earliest Albian, Middle–Late Albian, Late Albian–Early Cenomanian, and Mid Cenomanian) are marked by hardgrounds or dolomitic intervals. The planktonic biozones *Ticinella bejaouaensis, T. primula, T. praeticinensis*, *Rotalipora subticinensis, R. globotruncanoides* and *R. cushmani* co-occur with the following benthonic biozones: *Mesorbitolina texana* partial range zone, *M. subconcava* range zone, *Neoiraqia convexa* taxon-range zone, *Praealveolina iberica* interval zone and *Pseudedomia drorimensis* range zone. Within this biostratigraphic framework, a new carbon-isotope curve from the South Palmyrides was compared with $\delta^{13}C$ records of the Tethyan Realm and England that allows identifying several biotic events and Oceanic Anoxic Events (OAE), recorded in the Upper Albian to Upper Cenomanian succession. The combination of sequence-stratigraphic interpretations and comparisons, with our results have led to an improved understanding of the Cretaceous platform architecture of the South Palmyrides that links the Arabian Platform to the east with the Levant Platform to the southwest.

INTRODUCTION

Much progress has been made in the understanding of the Cretaceous sequence stratigraphy of the Arabian Plate (Sharland et al., 2001, 2004) and Levant Platform (Kuss et al., 2003; Homberg and Bachmann, 2010). In contrast, the Cretaceous stratigraphy of the Palmyrides in Syria, which lies between these two regions, is less well studied. The Palmyrides formed at the southwestern edge of the Neo-Tethys Ocean, which was isolated from the rest of the Arabian Platform by the Al-Hamad Uplift (Mouty, 1997). During the Late Aptian and Cenomanian they were characterized by the deposition of shallow-water carbonates, in addition to some Albian pelagic sediment. Surface exposures of Cretaceous sediments are located in the cores of anticlinal folds and dome-like structures of the South Palmyrides Chain (Krasheninnikov et al., 2005; Mouty et al., 1983; Ponikarov et al., 1966; Figure 1). These folds were cut by large faults that produce a scarp-and-cliff ridge landscape (Al-Maleh et al., 2000). The investigated area is located northeast of Damascus and extends approximately 15–17 km between the Admir and Zbeideh sections in the southwestern part of the South Palmyrides (Figures 1 and 2).

In most localities of the South Palmyrides, the Cretaceous units are formed by shallow-water carbonates including limestone or dolomites with intercalated marly beds (Krasheninnikov et al., 2005; Mouty et al., 1983; Ponikarov et al., 1966). These sediments accumulated in peritidal, tropical-water platform environments (Stampfli et al., 2001) with molluscs, foraminifera, echinoderms, ostracods and some green/red algae as major carbonate producers. We concentrated sampling to limestones (including marly and dolomitic limestone units). However, some intervals are strongly dolomitized and therefore lack biostratigraphically indicative fossils (Figure 3). The abundant and varied planktonic and benthonic foraminifera permit high-resolution biostratigraphic subdivision of the Aptian to Cenomanian strata from the South Palmyrides, supplemented by a detailed Late Albian to Middle Cenomanian carbon-isotope record.

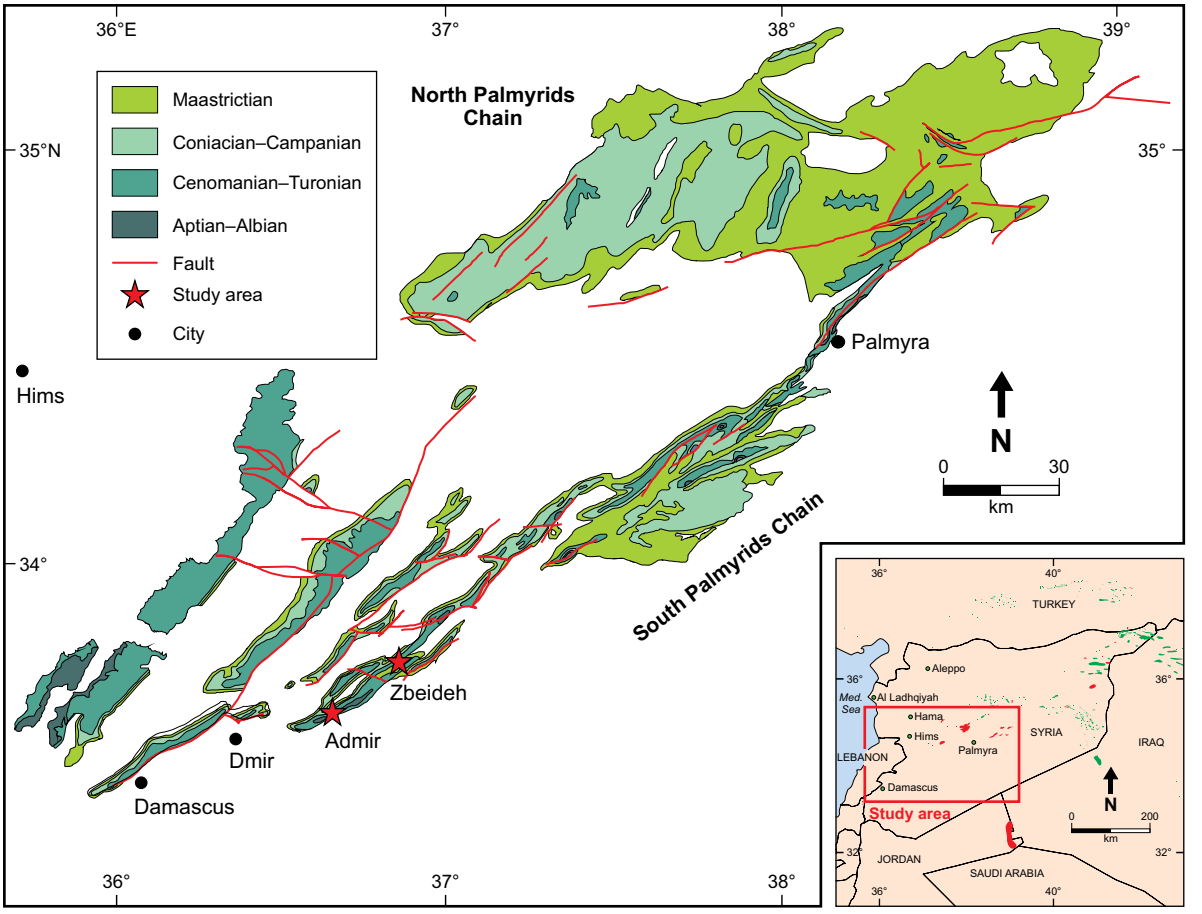

Figure 1: The Cretaceous outcrops of the Palmyrides, showing the locations of the Admir Section at latitudes 33°69'45"N and longitudes 36°86'55"E, and the Zbeideh Section at latitudes 33°78'36"N and longitudes 36°98'73"E.

METHODS

We analyzed microfacies and biostratigraphy based on 65 thin sections from the Admir Section, and 78 from the Zbeideh Section. However, not all thin sections could be used for biostratigraphic zonation because of dolomitization (Figure 3). The systematic identification of foraminifera is based on the schemes of various authors (Schroeder and Neumann, 1985; Caron, 1985; Loeblich and Tappan, 1988; Premoli Silva and Verga, 2004; Velić, 2007; Boudagher-Fadel, 2008). The biozone concepts used for the Palmyrides were correlated with those from other Tethyan areas proposed by the above-mentioned authors, as well as Ogg (2004a, b). Bulk rock samples (n = 103) for carbon-isotope analysis have been collected from the Admir Section (Figures 1 and 3). The curve of carbon-isotope data *versus* depth has been compared with trends derived from published carbon-isotope curves (Friedrich, 2010; Jarvis et al., 2006; Kennedy et al., 2004; Gale et al., 1996).

LITHOSTRATIGRAPHY

The lithostratigraphic subdivision of the here-considered siliciclastic Palmyra Sandstone Formation, and the Zbeideh and Abou-Zounnar carbonate formations follows Mouty et al. (1983).

Palmyra Sandstone Formation

The Palmyra Sandstone Formation (12 m thick) is composed of grayish claystones with thin sandstone intercalations and thin dolomitic marls at the top (Figure 3).

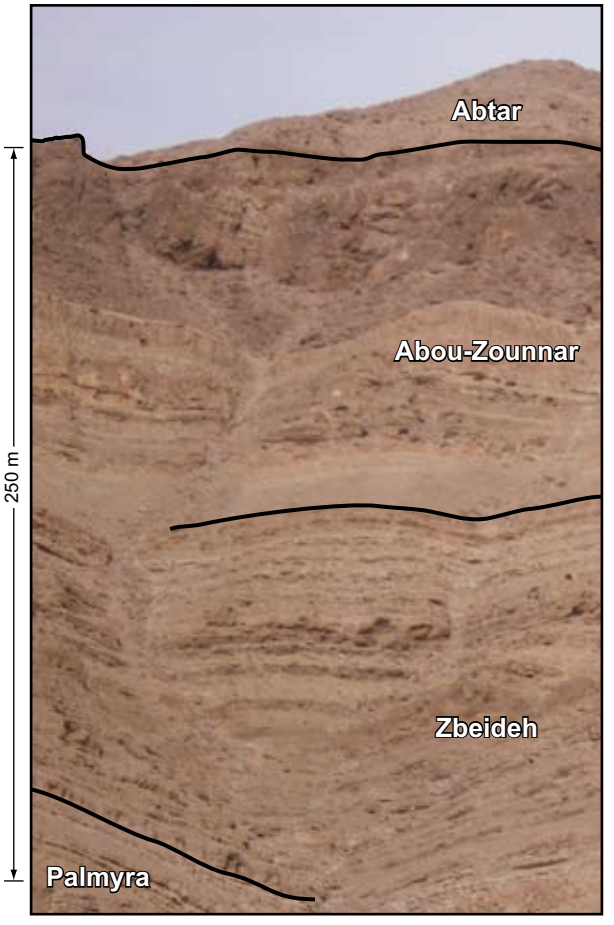

Figure 2: The studied succession of the Zbeideh Section with formation names.

Age: Most authors attributed an (?Barremian–Aptian) age for the Palmyra Sandstone Formation (e.g. Mouty et al., 2003).

Zbeideh Formation

Unit 1 is composed of massive limestones (packstones and wackestones with green algae, benthonic and planktonic foraminifera, and molluscs), intercalated with some marly limestones (rich in bivalves).
Unit 2 is composed of fossiliferous marly limestones (often rhythmic), intercalated with dolomitic limestones and dolomites.
Unit 3 is composed of unfossiliferous marly and massive dolomites, partly with moldic porosity and some quartz nodules.
Unit 4 consists of alternating dolomites and grayish dolomitic marls and intercalated with thin dolomitic limestones and soft green marls (with abundant bivalves). The upper part of unit 4 is restricted to the Admir Section and consists of fossiliferous white limestones (often nodular) with planktonic foraminifera, and intercalated nodular limestones (well-bedded) with marls rich in oysters.
Unit 5 is composed of fossiliferous massive limestones (packstones and wackestones with benthonic and planktonic foraminifera, and molluscs).

Age: Most previous authors attributed an Albian to Early Cenomanian age for the Zbeideh Formation (e.g. Mouty et al., 1983). Benthonic foraminifera of the lowermost limestones of unit 1, however, indicate a Late Aptian age (Figure 3).

Abou-Zounnar Formation

The Abou-Zounnar Formation above is up to 115 m thick and was subdivided into four units (Figure 3):

Unit 1 is represented by white limestones (mudstones and wackestones with benthonic foraminifera and red algae) and brownish dolomite with intercalations of fossiliferous grayish dolomarls and marly limestones.
Unit 2 is composed of green and gray marls with abundant oysters, intercalated with nodular thin to massive white dolomites and limestones (packstones and wackestones) with bivalves, gastropods, ostracods and some planktonic foraminifera.
Unit 3 is represented by green and gray marls with oysters, intercalated with foraminiferal limestone beds (the upper part of this unit marly gypsum).
Unit 4 forms cliff walls of massive dark brownish dolomite. Massive dolomites of the Abtar Formation overly this unit 5 (Figure 2).

Age: Mouty et al. (1983) suggested a Mid to Late Cenomanian age of the Abou-Zounnar Formation, which is confirmed by our data. The Cenomanian/Turonian boundary lies in the dolomites of the Abtar Formation above (based on interpretations of $\delta^{13}C$ values).

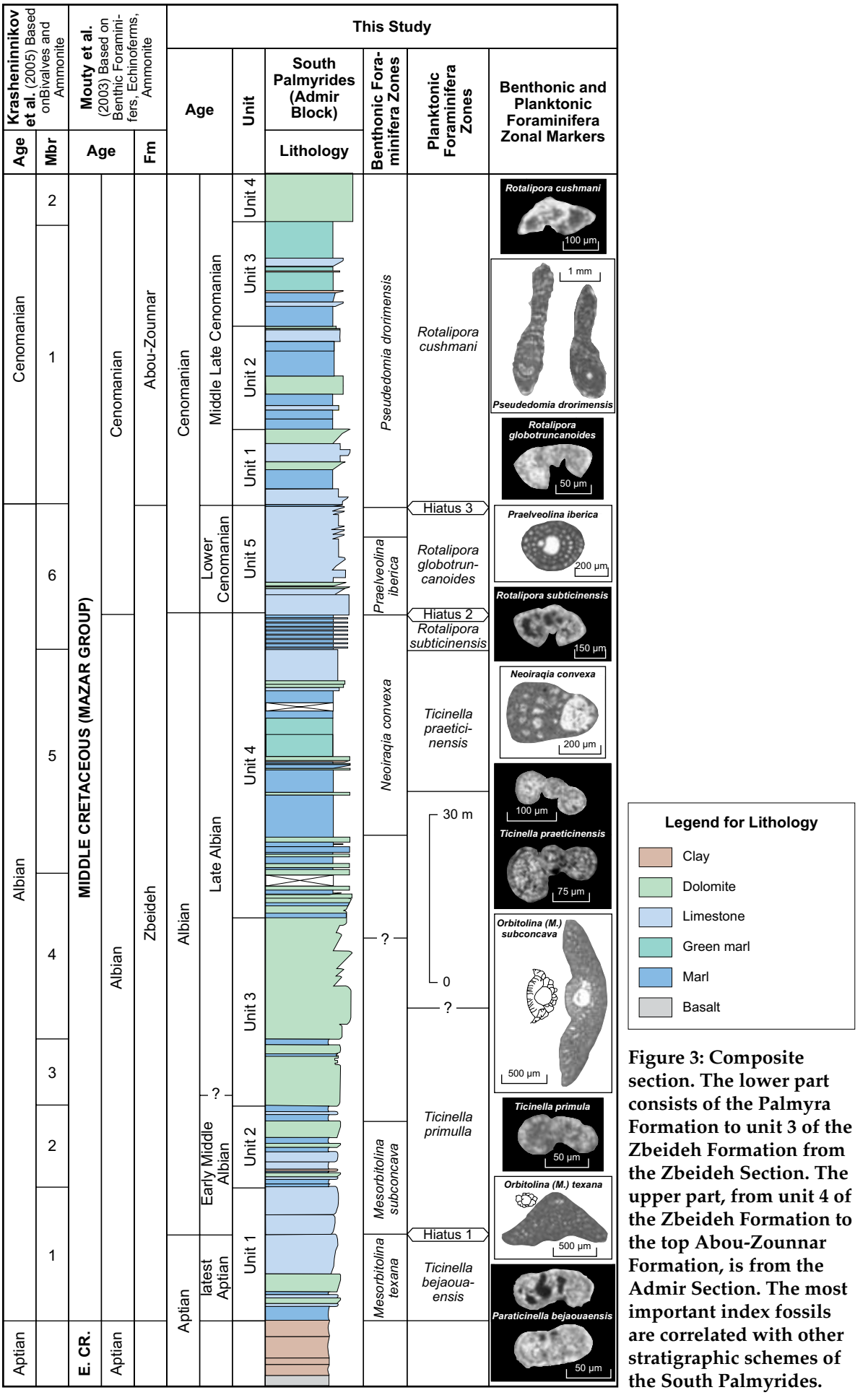

Figure 3: Composite section. The lower part consists of the Palmyra Formation to unit 3 of the Zbeideh Formation from the Zbeideh Section. The upper part, from unit 4 of the Zbeideh Formation to the top Abou-Zounnar Formation, is from the Admir Section. The most important index fossils are correlated with other stratigraphic schemes of the South Palmyrides.

BIOSTRATIGRAPHY

Our biostratigraphic subdivision is based on planktonic foraminifera and benthonic foraminifera (Late Aptian–Late Cenomanian) of both the Admir and Zbeideh sections from the South Palmyrides. Four major hiatuses are delimited, one around the Aptian/Albian boundary, the second around Middle/Late Albian, the third around the Albian/Cenomanian boundary and the fourth in the Middle Cenomanian (Figures 4).

Planktonic Foraminifera Biostratigraphy

The high variety of planktonic foraminifera allows defining six biozones, based on the first (FO) and last occurrence (LO) of several index taxa. They range from Late Aptian to Late Cenomanian and are well comparable to assemblages from the Tethyan Realm (Ogg, 2004a, b; Premoli Silva and Verga, 2004).

Paraticinella bejaouaensis zone

Diagnosis: Total range zone of *Paraticinella bejaouaensis* (Sigal, 1966).

Description: The limestones of that biozone are characterized by *Paraticinella bejaouaensis,* an Upper Aptian trochospiral index species (Premoli Silva and Verga, 2004, Premoli Silva, et al. 2009) associated with *Hedbergella mitra*, *H. trochoidea*, *H. infracretacea, H. gorbachikae* (Figures 4 and 5a).

Correlation: The described assemblage holds several index species of the *Ticinella bejaouaensis* zone (Ogg, 2004a; Premoli Silva and Verga, 2004).

Age and Occurrence*:* Premoli Silva and Verga (2004) and Ogg (2004b) attributed a latest Aptian age for that biozone. In the present study, the *T. bejaouaensis* biozone occurs in a 15-m-thick succession of marly limestones and limestones, corresponding with the lower part of unit 1 of the Zbeideh Formation in the Zbeideh Section. This succession is uncomfortably overlain by limestones with *Ticinella primula* (Lower Albian, according to Caron, 1985).

Hedbergella planispira zone

This biozone is missing and may be represented by two hardgrounds (Figures 3 and 4). We correlate this hiatus with a local unconformity described in the Palmyrid Aulacogene (Krasheninnikov et al., 2005), and regionally in the Levant Basin (Ferry et al., 2007; Segev and Rybakov, 2009).

Ticinella primula zone

Diagnosis: Total range zone of *Ticinella primula*.

Description: This zone is delineated by *Ticinella primula*, associated with *T. roberti* (Gandolfi, 1942), *Hedbergella planispira* and *Muricohedbergella delrioensis*. The microfauna of this interval are badly preserved due to dolomitization processes (Figures 3 and 4).

Correlation: The described planktonic assemblage correlates with the *Ticinella primula* zone according to Premoli Silva and Verga (2004) and Ogg (2004a).

Age and Occurrence: This biozone was attributed to the Early and Middle Albian according to Premoli Silva and Verga (2004) and Ogg (2004a). *T. primula* (Figure 5b) appears in the Zbeideh Section in two massive limestone beds (9 m) of the upper part of unit 1 (Zbeideh Formation), directly above two hardgrounds that overlie limestones with *Paraticinella bejaouaensis* (Figure 4). The upper part of the *T. primula* biozone is missing because of dolomitization processes. The total thickness of this biozone may reach about 60 m (upper part of unit 1, units 2 and 3).

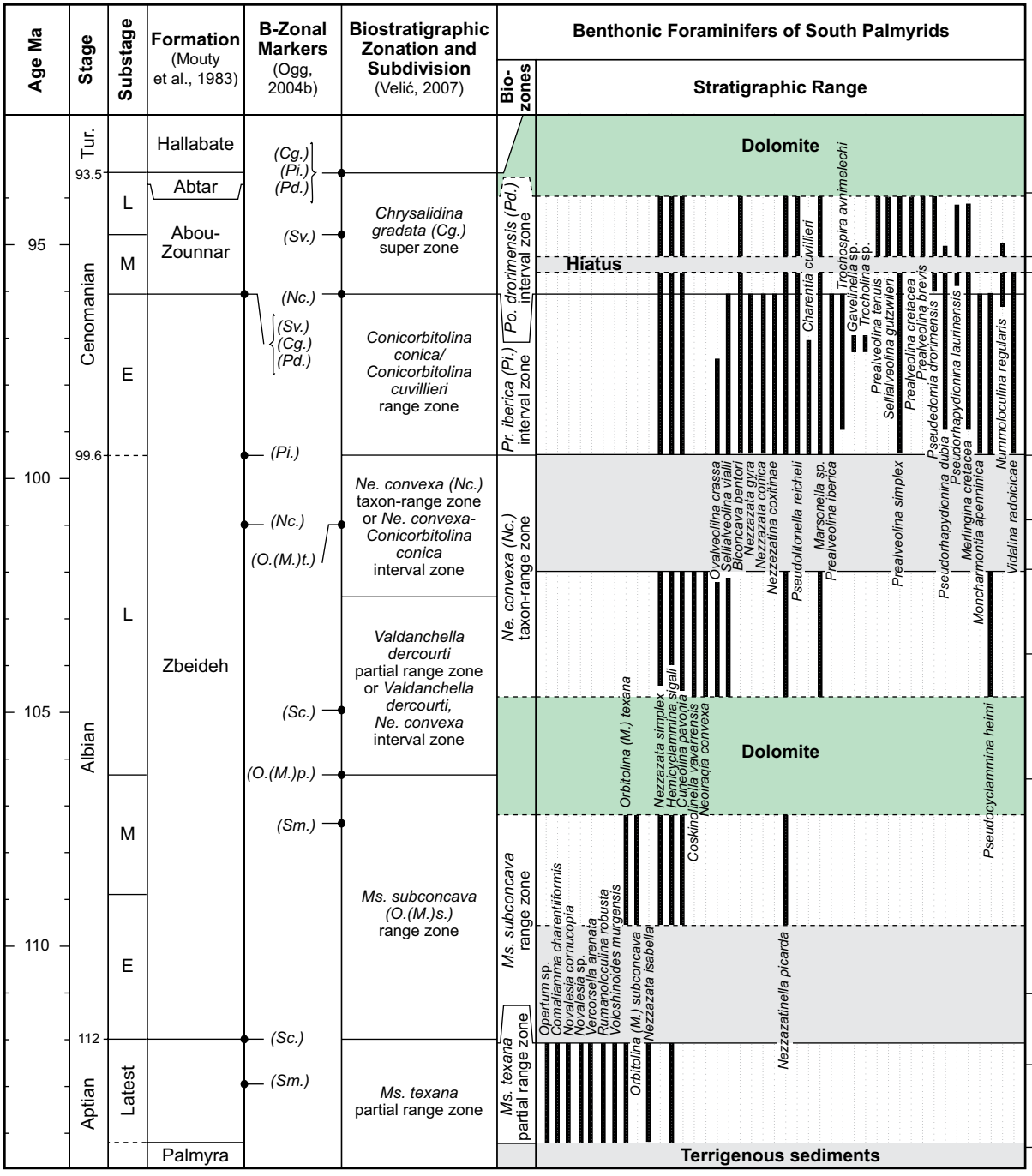

Genus abbreviations

Benthonic

B. = *Biconcava*
Ch. = *Charentia*
Cm. = *Comaliamma*
Co. = *Coskinolenella*
Cu. = *Cuneolina*
H. = *Hemicyclammina*
Mo. = *Moncharmontia*
Mr. = *Merlingina*
Ms. = *Mesorbitolina*
Ne. = *Neoiraqia*
Nl. = *Nezzazatinella*
Nn. = *Nezzazatina*
No. = *Novalesia*
Nu. = *Nummoloculina*
Nt. = *Nezzazata*
O. = *Ovalveolina*
Pc. = *Pseudocyclammina*
Ph. = *Pseudorhapydionina*
Pl. = *Pseudolituonella*
Po. = *Pseudedomia*
Pr. = *Prealveolina*
S. = *Sellialveolina*
R. = *Rumanoloculina*
T. = *Trochospira*
Ve. = *Vercorsella*
Vo. = *Voloshinoides*

Planktonic

B. = *Biticinella*
D. = *Dicarinella*
G. = *Globigerinelloides*
Hd. = *Hedbergella*
Ht. = *Heterohelix*
Ma. = *Macroglobigerinelloides*
Mu. = *Muricohedbergellaa*
Pr. = *Praeglobotruncana*
Pa. = *Paraticinensis*
R. = *Rotalipora*
T. = *Ticinella*
W. = *Whiteinella*

Abbreviations *sensu* Ogg (2004)

Cg. = *Chrysalidina gradata*
Hp. = *Hedbergella planispira*
Nc. = *Neoiraqia convexa*
O.(M).p. = *Mesorbitolina parva*
O.(M.)s. = *Mesorbitolina subconcava*
O.(M.)t. = *Mesorbitolina texana*
Pd. = *Pseudedomia drorimensis*
Pi. = *Prealveolina iberica*
Sm. = *Simplorbitolina manasi*
Sc. = *Simplorbitolina conulus*
Sv. = *Sellialveolina viallii*
Tb. = *Ticinella bejaouaensis*

Figure 4: *See facing page for contination.*

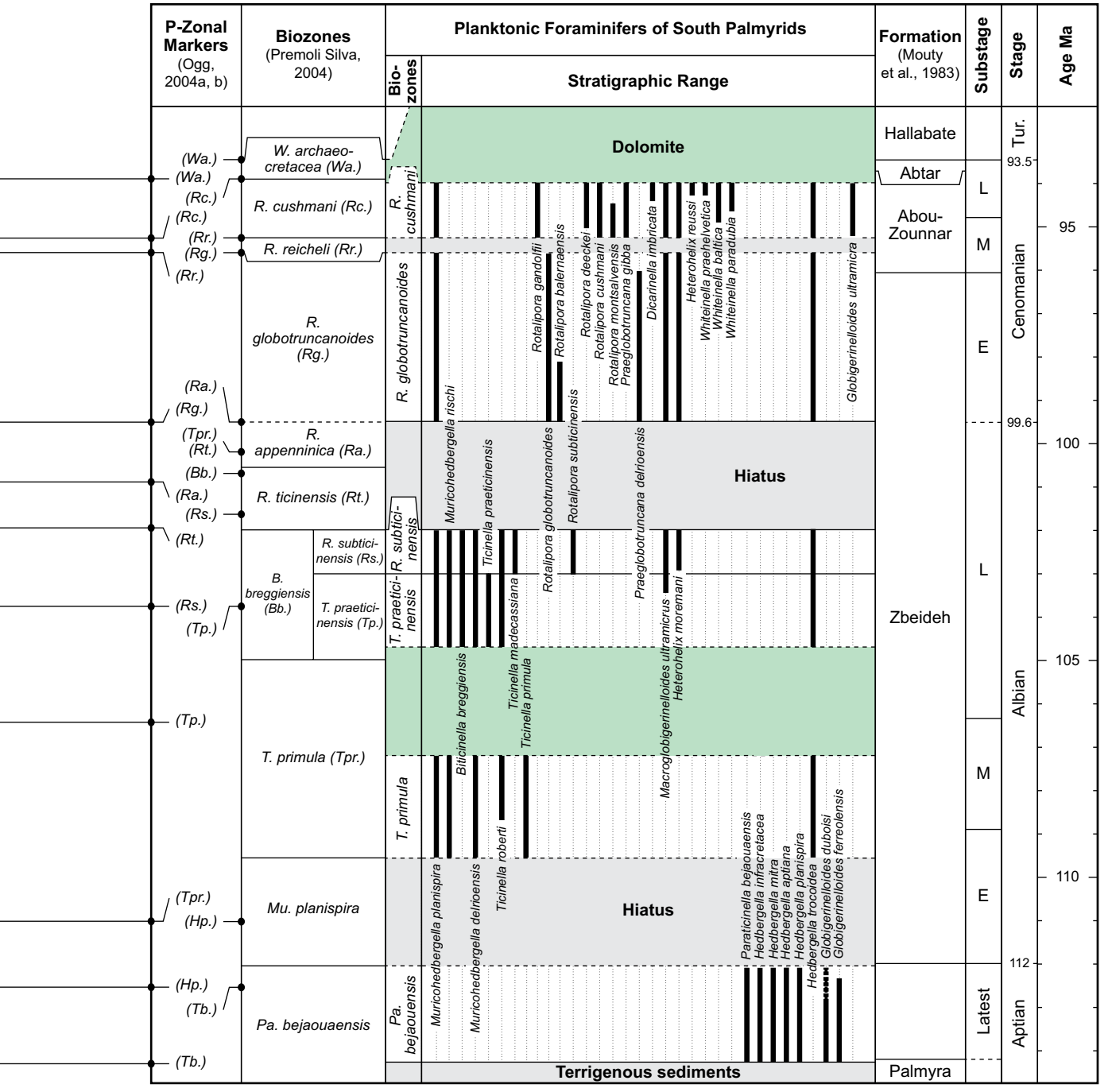

Figure 4 *(continued)*: Stratigraphic concepts and standard biozones (benthonic and planktonic foraminifera) in the South Palmyrides. Shaded areas indicate hiatuses or dolomitized intervals.

Ticinella praeticinensis zone

Diagnosis*:* Interval zone comprising the range between the FO of the zonal marker to the FO of *Rotalipora subticinensis* (Ogg, 2004a).

Description: Besides the zonal marker species, the following taxa characterize the *T. praeticinensis* interval zone: *T. roberti, Biticinella breggiensis, Muricohedbergella planispira, M. rischi* and *M. delrioensis.* The conspicuous increase in diversity and abundance is a further characteristic of that zone (Premoli Silva and Verga, 2004) (Figures 4 and 5c).

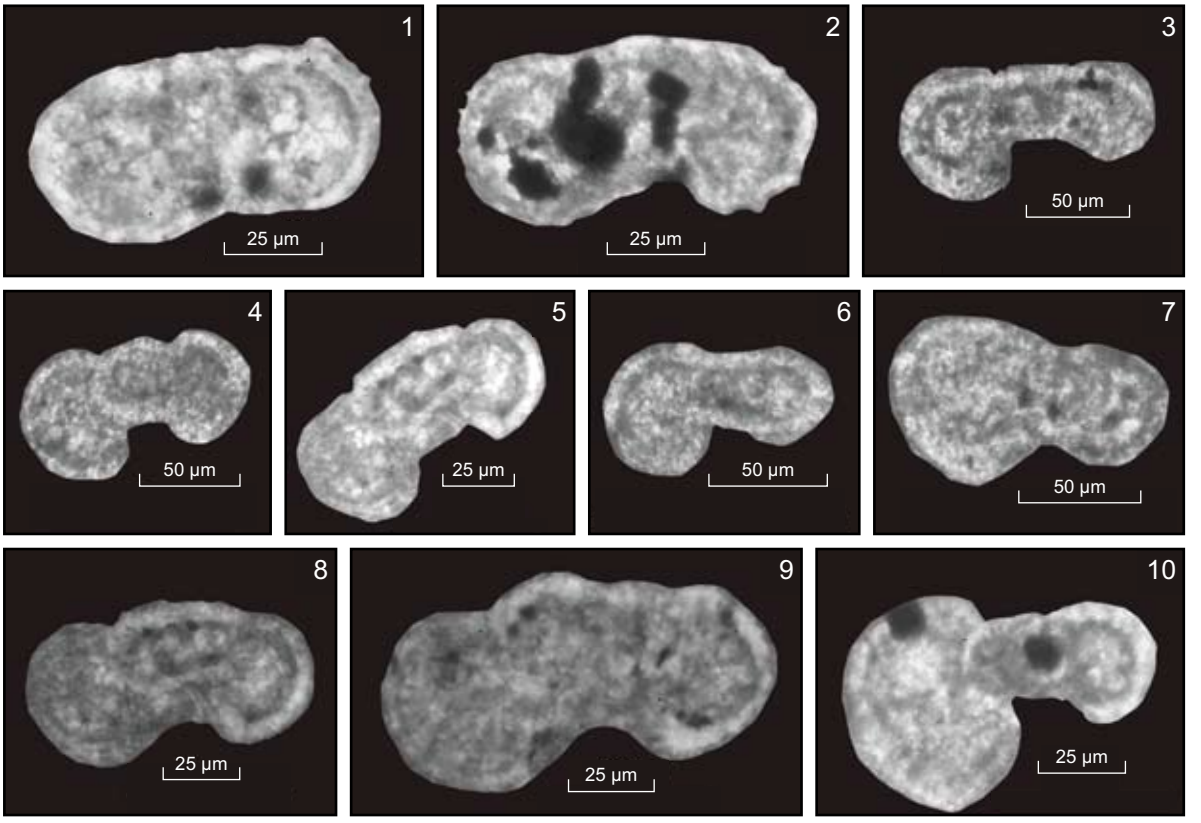

Figure 5a: Planktonic foraminifera of Late Aptian *Paraticinella bejaouaensis* zone: (1 and 2) *Paraticinella bejaouaensis* (Zbeideh); (3 to 9) *Hedbergella* cf. *aptiana* (Zbeideh); (4) *Hedbergella mitra* (Zbeideh); (5) *Hedbergella trochoidea* (Zbeideh); (6 and 7) *Hedbergella infracretacea* (Zbeideh); (8) *Hedbergella* sp. (Zbeideh); (10) *Hedbergella gorbachikae* (Zbeideh). Note: 1 to 5, and 7 to 10 are axial sections, 6 is a subaxial section.

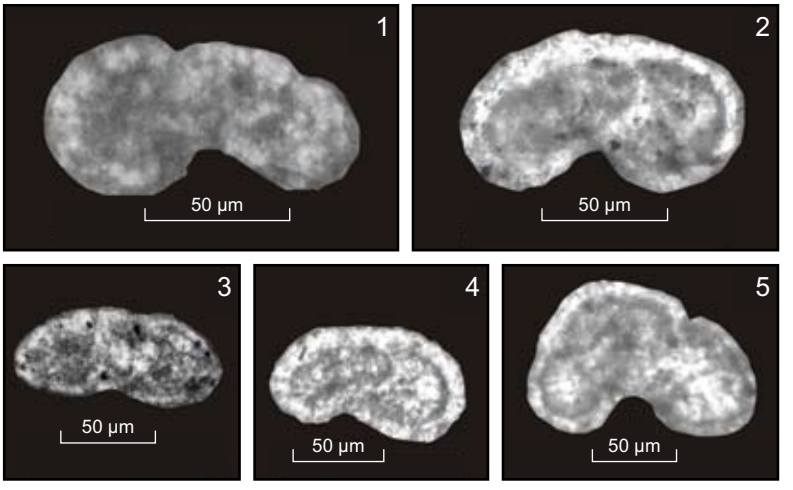

Figure 5b: Planktonic foraminifera of of Early Albian *Ticinella primula* zone: (1, 2 and 4) *Ticinella primula* (Zbeideh); (3) *Muricohedbergella delrioensis* (Zbeideh); (5) *Ticinella roberti* (Zbeideh). Note: 1 and 4 are axial sections. 2, 3 and 5 are subaxial sections.

Figure continued on facing page.

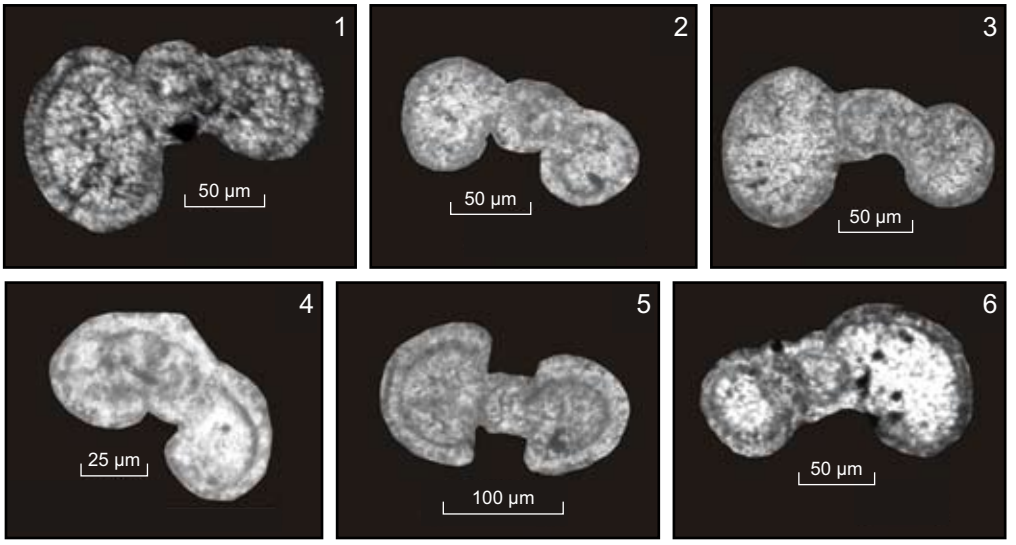

Figure 5c: Planktonic foraminifera of Late Albian *Ticinella praeticinensis* zone: (1 and 2) *Ticinella praeticinensis* (Admir); (3) *Muricohedbergella planispira* (Admir); (4 to 6) *Ticinella roberti* (Admir); (5) *Biticinella breggiensis* (Admir). Note: 1 to 6 are axial sections.
Figure continued on next page.

Correlation: Both, the marker species and the plankonic assemblage correlate with the *Ticinella praeticinensis* zone, defined by Ogg (2004a).

Age and Occurrence: This biozone corresponds to the Late Albian (Caron, 1985; Premoli Silva and Verga, 2004; Ogg, 2004a). It was defined in nodular limestones of unit 4 (Zbeideh Formation) of the Admir and Zbeideh sections (Figure 3), with the FO of *Ticinella praeticinensis* and *Biticinella breggiensis* at the base and the FO of *Rotalipora subticinensis* at the top (Ogg, 2004a).

Rotalipora subticinensis zone

Diagnosis*:* Total range zone of the zonal marker (Ogg, 2004a).

Description: The following planktonic foraminifera co-occur together with the zonal marker: *Biticinella breggiensis, Muricohedbergella delrioensis, M. rischi, M. planispira, Ticinella roberti* and *T. madecassiana* (Figure 4). This biozone marks the onset of species with keeled peripheries (Premoli Silva and Verga, 2004) (Figure 5d).

Correlation: The *Rotalipora subticinensis* zone (Ogg, 2004a) may be correlated with the upper part of the *Ticinella praeticinensis* and *Rotalipora subticinensis* subzone (Premoli Silva and Verga, 2004).

Age and Occurrence: The *R. subticinesis* zone was attributed a Late Albian age according to Ogg (2004a) and Premoli Silva and Verga (2004). It was determined in (6.2 m) thick nodular limestones of unit 4 of the Zbeideh Formation (Admir Section), based on the FO of *R. subticinensis* (Figures 3, 4 and 5d).

Rotalipora ticinensis and *Rotalipora appenninica* biozones

There is no evidence for these two biozones in the studied sections. We therefore assume a major hiatus at the Albian/Cenomanian boundary, confirmed by a major hardground at the base of unit 5 of the Zbeideh Section (Figure 3). The LO of *R. subticinensis* (at the top of unit 4) is followed by the FO of *R. globotruncanoides* (limestones of unit 5) and thus account for a hiatus between both biozones, comprising the *R. ticinensis* and *R. appenninica*. Based on age estimates given by Ogg (2004a), this hiatus spans ca. 2.4 million years (Figure 4).

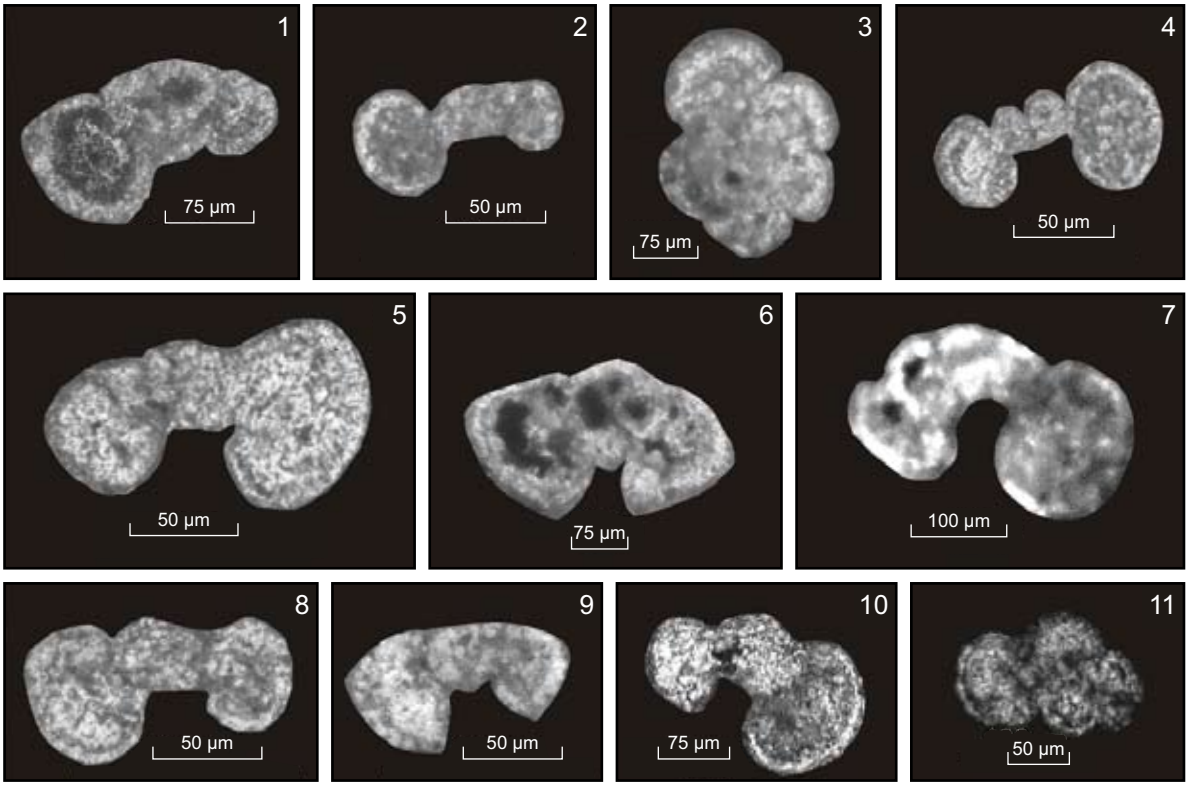

Figure 5d: Planktonic foraminifera of Late Albian to Early Cenomanian *Rotalipora subticinensis* zone and *Rotalipora globotruncanoides* zone: (1 and 6) *Rotalipora subticinensis* (Admir);(2) *Muricohedbergella planispira* (Zbeideh); (3) *Ticinella madecassiana* (Admir); (4) *Foraminifera* sp. (Admir); (5) *Muricohedbergella rischi* (Admir); (7) *Muricohedbergella rischi* (Zbeideh); (8) *Muricohedbergella delrioensis* (Admir); (9) *Rotalipora* cf. *globotruncanoides* (Admir); (10) *Muricohedbergella delrioensis*; (11) *Heterohelix* cf. *moremani* (Admir); Note: 1, 4 to 6, and 8 are axial sections. 2, 7, and 9 to 11 are subaxial sections. 3 is a subequatorial section.
Figure continued on facing page.

Rotalipora globotruncanoides zone

Diagnosis*:* Total range zone of the zonal marker (Ogg, 2004a).

Description: The following planktonic foraminifera co-occur together with the zonal marker: *Ticinella madecassiana*, *Praeglobotruncana delrioensis, Muricohedbergella delrioensis* and *Heterohelix moremani.* Benthonic foraminifera are more frequent during that interval (Figures 3, 4 and 5d).

Correlation: The described planktonic assemblage equals with the zonal marker of the standard global planktonic event (Ogg, 2004a, b) (compare Figures 3 and 4).

Age and Occurrence: The *R. globotruncanoides* biozone correlates with the Early Cenomanian (Premoli Silva and Verga, 2004; Ogg, 2004a). It occurs in thick-bedded limestone of the uppermost part of the Zbeideh Formation. The base of this biozone is delineated by the FO of *R. globotruncanoides* – its top by the FO of *R. gandolfii*. (Figures 3 and 4)

Rotalipora reicheli zone

A hardground surface between the LO of *Rotalipora globotruncanoides* and the FO of *R. cushmani* coincides with a stratigraphical gap that represents the *Rotalipora reicheli* zone of the Middle Cenomanian (between 97 to 96.6 Ma, Ogg, 2004a).

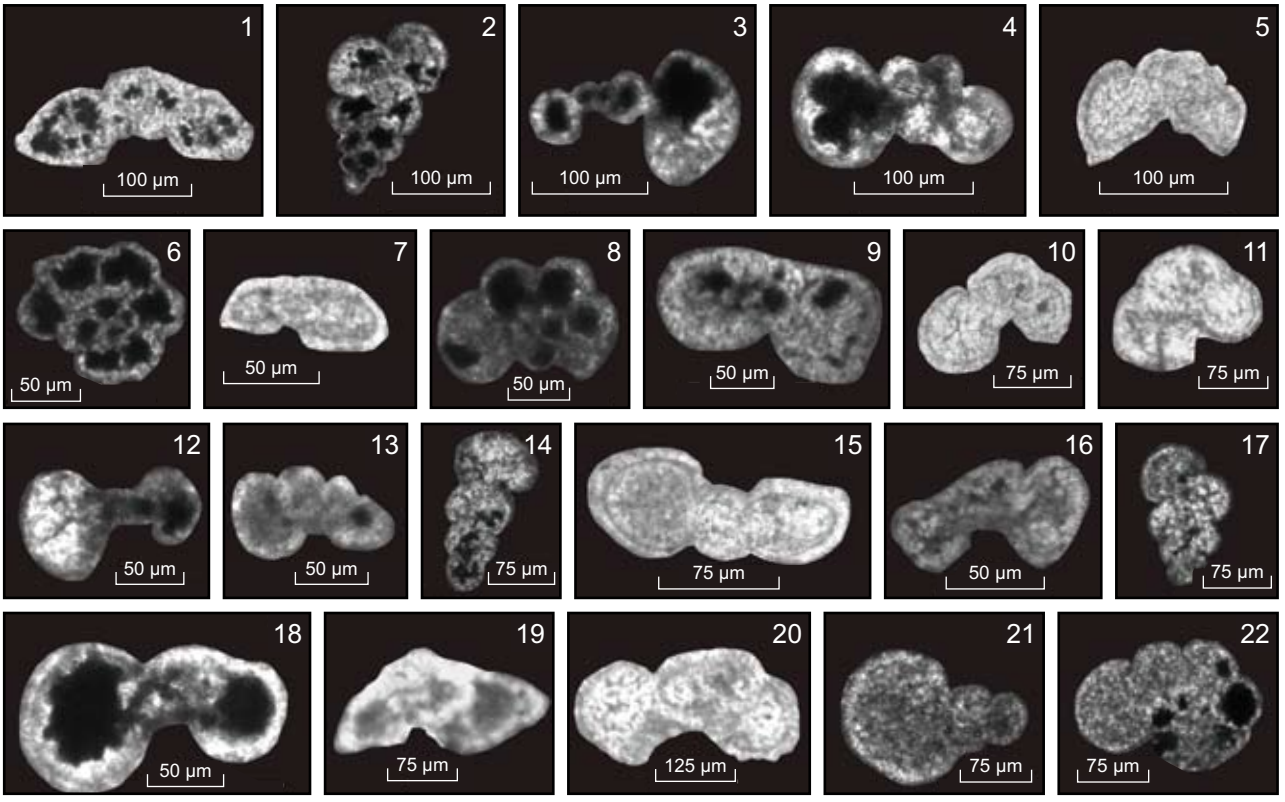

Figure 5e: Planktonic foraminifera of Late Cenomanian *Rotalipora cushmani* zone: (1) *Dicarinella imbricata* (Admir); (3 and 15) *foraminifera* sp. (Admir); (2 and 14) *Heterohelix reussi* (Zbeideh); (4 and 20) *Whiteinella baltica* (Zbeideh); (5) *Praeglobotruncana gibba* (Admir); (6) *Macroglobigerinelloides ultramicra* (Zbeideh); (7) *Rotalipora* cf. *montsalvensis* (Admir); (8) *Hedbergella planispira* (Zbeideh); (9) *Hedbergella simplex* (Admir); (10 and 11) *Whiteinella* cf. *paradubia* (Admir); (12) *Macroglobigerinelloides* sp. (Zbeideh); (13 and 16) *Hedbergella* sp. (Zbeideh); (17) *Heterohelix moremani* (Zbeideh); (18) *Whiteinella praehelvetica* (Zbeideh); (19) *Rotalipora* cf. *cushmani* (Admir); (21 and 22) *Globigerinelloides ultramicra* (Zbeideh); Note: 1 to 4, 10, 17, 18 and 20 are axial sections. 5, 7, 9, 11 to 16, 19, 21 are subaxial sections. 6 and 22 are equatorial sections. 8 is a subequatorial section.

Rotalipora cushmani zone

Diagnosis*:* Total range zone of the zonal marker (Ogg, 2004a).

Description: Numerous keeled taxa occur in this biozone, which is characterized by *R. cushmani* associated with *Globigerinelloides ultramicra, Dicarinella algeriana, D. imbricata, Praeglobotruncana gibba, Whiteinella paradubia, W. praehelvetica, W. baltica, W. aumalensis, Heterohelix moremani, H. reussi, Rotalipora gandolfii, R. deeckei* and *R. montsalvensis.* Keeled taxa become more abundant and slightly bigger towards the middle part of this biozone and gradually disappear towards the upper part. The genus *Whiteinella* is more common in the upper part of this zone (Figures 4, 5e and 6).

Correlation: The described planktonic assemblage correlates with the *Rotalipora cushmani* zone according to Premoli Silva and Verga (2004) and Ogg (2004a) (Figure 4).

Age and Occurrence: The *R. cushmani* biozone corresponds to the Late Cenomanian (Premoli Silva and Verga, 2004; Ogg, 2004a) (Figure 4). It is determined in the Zbeideh Section based on the FO of *R. cushmani* and *R. deeckei* (Figure 6) and in the Admir Section, based on the LO of *R. gandolfii* and the FO of *R. cushmani* (Figures 3 and 4). The *R. cushmani* zone is evident in marly limestones, alternating with limestones and dolomites (ca. 40 m thick) of units 1, 2 and 3 of the Abou-Zounnar

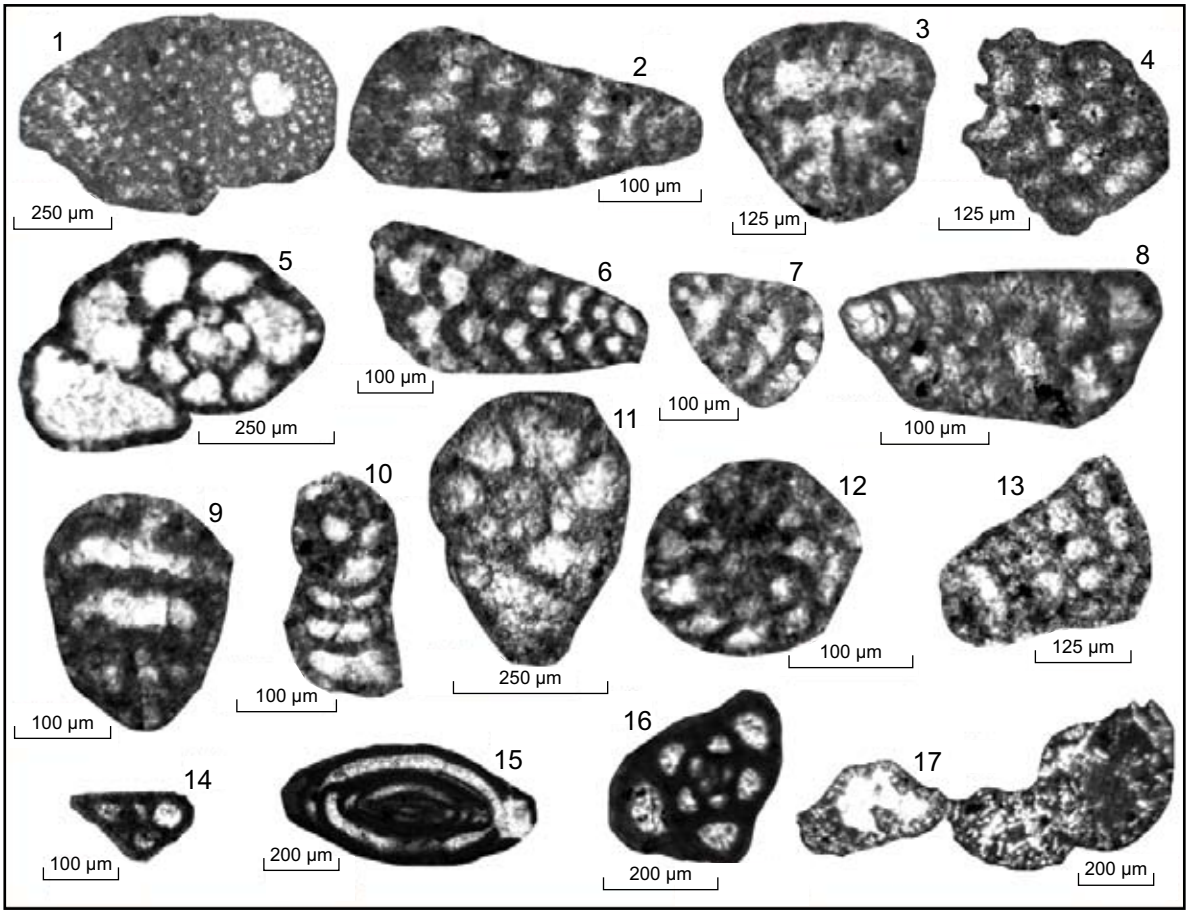

Figure 6a: Benthonic foraminifera of the Late Aptian *Mesorbitolina texana* partial range zone: (1 and 4) *Mesorbitolina texana*, (1) [ob] through a young megalospheric form, (4) [sas]. (2, 3, 7 and 13) *Vercorsella arenata*, (2 and 13) [sas], (3 and 7) [ts] (4, 14 and 17) foraminifera sp. (Zbeideh). (5 and 11) *Comaliamma charentiiformis*, (5) [sas], (11) [es] (Zbeideh). (9) *Opertum* sp. [ts] (Zbeideh). (6 and 8) *Novalesia cornucopia*, [sas] (Zbeideh). (10) *Novalesia* sp., [sas] (Zbeideh). (12) *Nezzazata isabella* [ses] (Zbeideh). (16) *Rumanoloculina robusta*, [sas] (Zbeideh). (15) miliolid indet. (Zbeideh), (Admir). Abbreviations: as = axial section; sas = subaxial section; es = equatorial section; ses = subequatorial section; ob = oblique section; ts = transversal section; ls = longitudinal section.
Figure continued on facing page.

Formation of the Admir Section, corresponding to units 2 and 3 of Abou-Zounnar Formation of the Zbeideh Section (ca. 75 m thick).

Benthonic Foraminifera Biostratigraphy

Numerous benthonic foraminifera are useful index fossils of the Cretaceous carbonate platforms (Boudagher-Fadel, 2008). They show a widespread distribution, high diversity and abundance in the studied sections of the South Palmyrides (Figures 6a to 6e), and thus are important for the biostratigraphic subdivision. Based on the concepts of Velić (2007), Ogg (2004b), and Schroeder et al. (2010), the following five biozones (overlapping most planktonic zonal boundaries; Figure 4) were defined.

Mesorbitolina texana zone (Velić, 2007)

Diagnosis: The base of this partial range zone has been determined by the FO of the zonal marker. The top corresponds to the FO of *Mesorbitolina subconcava*.

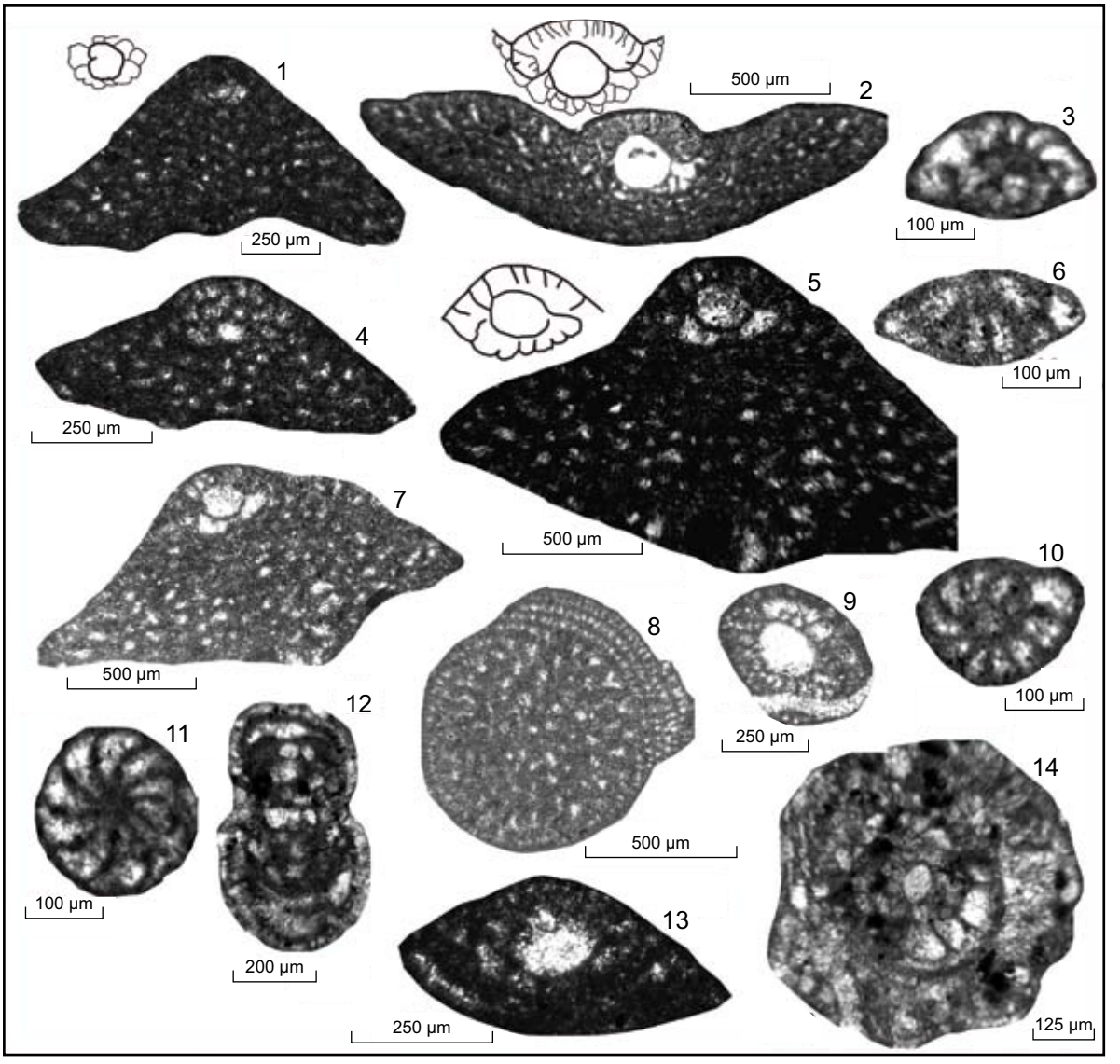

Figure 6b: Benthonic foraminifera of Early Albian *Mesorbitolina subconcava* zone: (1 and 4) *Mesorbitolina texana*, [as] (Zbeideh). (6, 10 and 11) *Nezzazata isabella*, (6) [sas], [ses] (Zbeideh). (8) *Orbitolina* sp. [ts] (Zbeideh). (3) *Nezzazata simplex* [sas] (Zbeideh). (2, 5, 7, 9 and 13) *Mesorbitolina subconcava*, [as] (Zbeideh). (12 and 14) *Hemicyclammina sigali*, (12) [as] (Admir), (14) [es] (Zbeideh). Abbreviations: as = axial section; sas = subaxial section; es = equatorial section; ses = subequatorial section; ob = oblique section; ts = transversal section; ls = longitudinal section.
Figure continued on next page.

Description: *M. texana* spans a long stratigraphic interval, ranging from the mid Late Aptian to the Middle Albian (Loeblich and Tappan, 1988; Velić, 2007). In addition to the zonal marker species, the following taxa occur within the *M. texana* biozone of the present study**:** *Voloshinoides murgensis*, *Opertum* sp., *Novalesia cornucopia, Comaliamma charentiiformis, Vercorsella arenata, Novalesia* sp., *Rumanoloculina robusta, Nezzazata isabellae,* including few miliolids and agglutinated foraminifera (Figures 4 and 6a).

Correlation: The described benthonic assemblage correlates with the *Mesorbitolina texana* partial range zone of the Adriatic platform, described by Loeblich and Tappan (1988) and Velić (2007).

Age and Occurrence*:* The *M. texana* zone indicates a latest Aptian age (Figures 3 and 4), documenting the first benthonic foraminifera in the Cretaceous succession of the South Palmyrides.

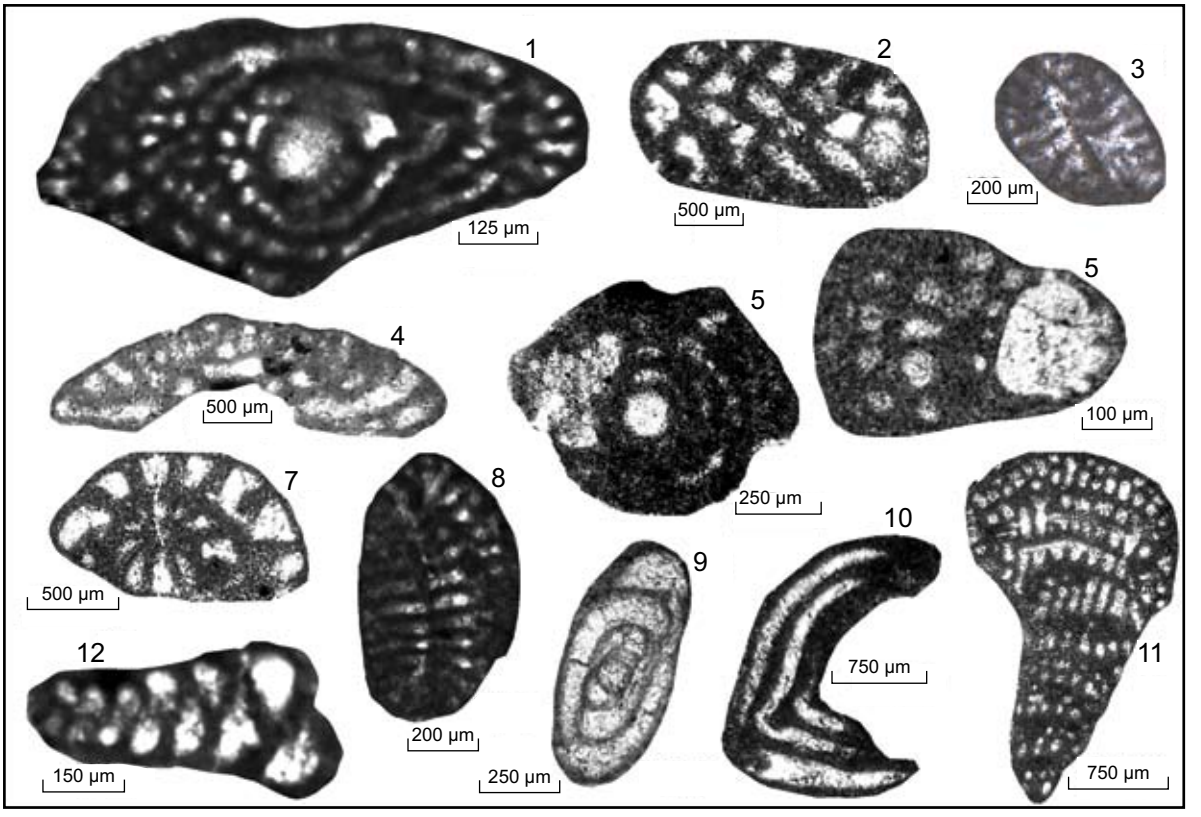

Figure 6c: Benthonic foraminifera of Late Albian *Neoiraqia convexa* taxon-range zone: (1) *Sellialveolina viallii*, [as] (Admir). (2) *Coskinolinella* sp.,? [ts], microspheric form (Admir). (3, 8 and 11) *Cuneolina pavonia*, (3) [ts], (8 and 11) [sas] (Admir). (4) *Coskinolinella navarrensis*, [os] (Admir). (5) *Ovalveolina crassa*, [es] (Admir). (6) *Neoiraqia convexa*, [os] young megalospheric form (Admir). (7) *Nezzazata simplex* [ses] (Admir). (9) miliolid indet. (Admir). (10) *Pseudonummoloculina heimi* (Admir). (12) *Novalesia* sp. [sas] (Admir). Abbreviations: as = axial section; sas = subaxial section; es = equatorial section; ses = subequatorial section; ob = oblique section; ts = transversal section; ls = longitudinal section.
Figure continued on next page.

It is recorded from 15-m-thick marly limestones and limestones, representing the lower part of unit 1 (Zbeideh Formation) in the Zbeideh Section (Figures 3 and 4). According to Velić (2007) the *M. texana* zone is defined by the total range of *Voloshinoides murgensis* or by the interval between the FO of *V. murgensis* and *Novalesia* sp. to the FO of *Mesorbitolina subconcava*.

Mesorbitolina subconcava zone

Diagnosis: Total range zone of the zonal marker (Velić, 2007).

Description: Besides the zonal marker, additional foraminifera (known as Albian index taxa) occur, such as *Nezzazata*, *N. simplex*, *Hemicyclammina sigali*, and *Nezzazatinella picardi* plus some miliolids and *M. texana* (Figures 4 and 6b).

Correlation: The benthonic foraminifera assemblage described coincides with *Mesorbitolina subconcava* zone of Velić (2007) (Figure 4).

Age and Occurrence: The *M. subconcava* zone comprises the Early to Middle Albian (Velić, 2007). Our planktonic biozonation confirms the FO of *M. subconcava* in the Lower Albian (Figure 4) in contrast to Schroeder et al. (2010), who discuss an earlier appearance of the zonal marker.

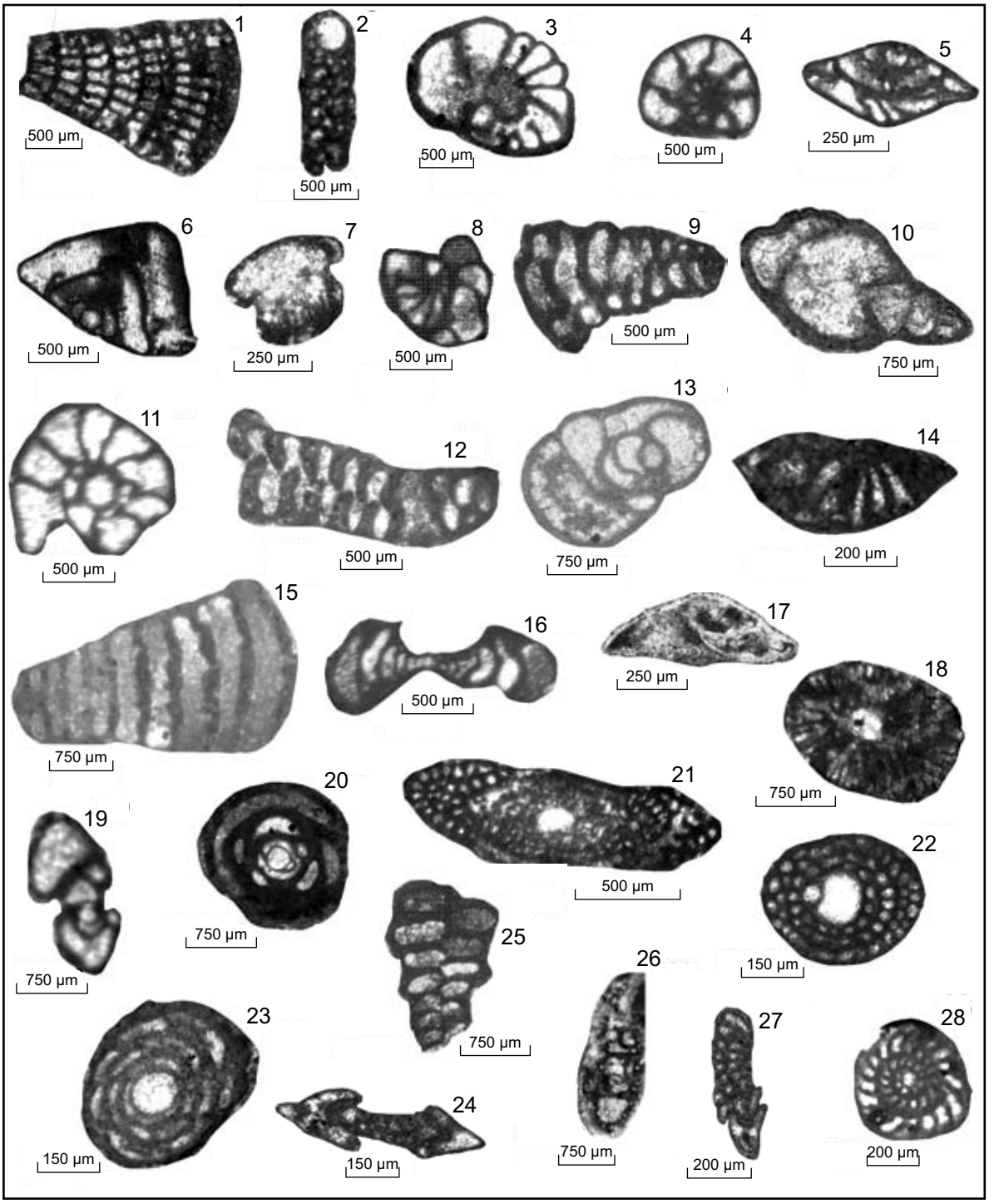

Figure 6d: Benthonic foraminifera of Early Cenomanian *Praealveolina iberica* interval zone: (1 and 2) *Cuneolina pavonia*, [os] through a young megalospheric form, (3) *Nezzazatinella picardi* [sas] (Zbeideh), (4 and 8) *Nezzazata simplex*, [ses] (Admir), (25) [sas] (Zbeideh). (5) *Nezzezata gyra*, [as] (Zbeideh). (6) *Nezzazata conica*, [as] (Admir). (7) *Trocholina* sp. (Admir). (9 and 15) *Pseudolituonella reicheli*, [ls] (Admir). (10 and 13) *Peneroplis* sp., (Admir). (11) *Moncharmontia apenninica*, [es] (Admir). (12) *Novalesia* cf. [as] (Admir). (14) *Trochospira avnimelechi*, [sas] (Zbeideh). (16) *Nummoloculina regularis*, [sas] (Admir). (17) *Gavelinella* sp. (Admir). (18) *Dictyopsella* sp.,? [ts] (Admir). (19) *Moncharmontia apenninica*, [as] (Admir). (20) *Miliolid* sp. [as] (Admir). (21) S*ellialveolina viallii*, [as] (Admir). (22 and 23) *Praealveolina iberica*, (22) [os] of megalospheric form (Admir), (23) Slightly [os] (Z). (24, 27 and 28) *Biconcave bentori*, (27) [sas] (Admir), (28) [es] (Zbeideh), (25) *Marssonella* sp. [sas] (Admir). (26) *Charentia cuvillieri*, slightly [as] (Admir). Abbreviations: as = axial section; sas = subaxial section; es = equatorial section; ses = subequatorial section; ob = oblique section; ts = transversal section; ls = longitudinal section.

Figure continued on next page.

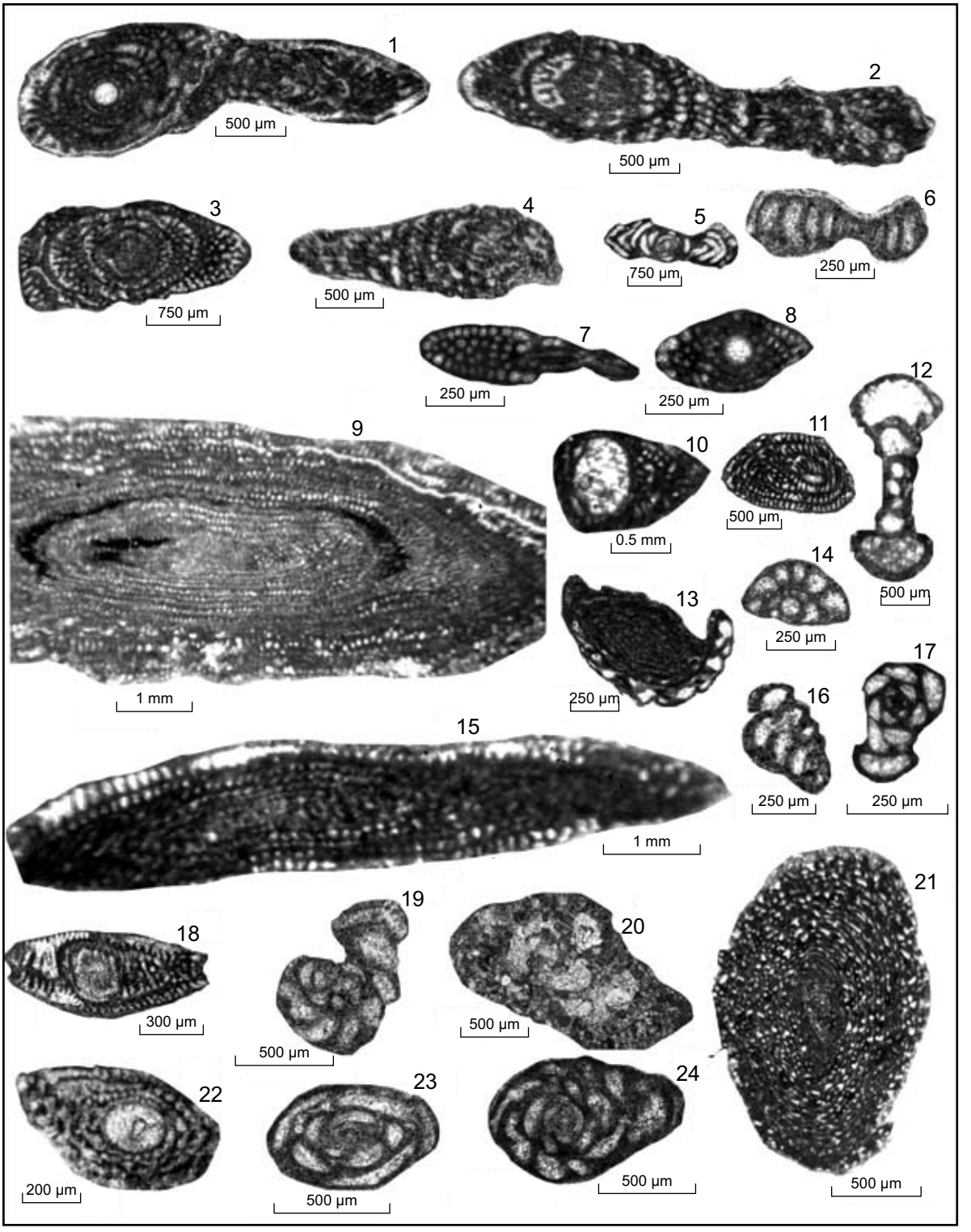

Figure 6e: Benthonic foraminifera of Late Cenomanian *Pseudedomia drorimensis* range zone: (1 to 4) *Pseudedomia drorimensis*, (1) [as], (2 to 4) [sas] (Admir). (5) *Pseudocyclammina heimi*, [as] (Admir). (6) *Nummoloculina regularis*, [sas] (Zbeideh). (7 and 8) *Sellialveolina* sp., (7) [sas], (8) [as] (Admir). (9, 10, 15, 18, 21 and 25) *Praealveolina tenuis*, (9, 21 and 25) [sas], (9) (Admir), (21 and 25) (Zbeideh), (10 and 18) [as] (Zbeideh). (11) *Praealveolina simplex*, [sas] (Zbeideh). (12 and 20) *Hemicyclammina* sp., (12) [as], (20) [ses] (Admir). (13 and 22) *Praealveolina cretacea*, 13 [sas] (Zbeideh), (22) [as] (Admir). (14) *Nezzazata simplex* [sas] (Zbeideh). (16) foraminifera sp., (19 to 24) *Pseudorhapydionina dubia*, [as] (Admir). (17 and 23) miliolid indet. (Admir). Abbreviations: as = axial section; sas = subaxial section; es = equatorial section; ses = subequatorial section; ob = oblique section; ts = transversal section; ls = longitudinal section.

The *M. subconcava* biozone was evidenced in 12-m-thick limestones of the Zbeideh Formation (Zbeideh Section, Figure 7), spanning the upper part of unit 1 and nearly all of unit 2. Its base is defined by the FO of *M. subconcava,* while the upper boundary of this biozone is missing due to strong dolomitization processes. The dolomitization also affected the lower part of *Neoiraqia convexa* biozone (Figures 3 and 4).

Neoiraqia convexa taxon-range zone

Diagnosis*:* Total range zone of zonal marker (Velić, 2007).

Description: This biozone is defined by the index fossil *Neoiraqia convexa,* associated with *Coskinolinella navarrensis, Ovalveolina crassa* and *Sellialveolina viallii*. Moreover, further taxa of wide stratigraphic range like *Cuneolina pavonia, Nezzazata simplex, Pseudocyclammina heimi, Novalesia* sp. and some miliolids occur in that biozone (Figures 4 and 9c).

Correlation: The *Neoiraqia* biozone correlates with the upper part of *Valdanchella dercourti* partial range zone and *Neoiraqia convexa* taxon-range zone proposed by Velić (2007). Moreover, it is characterized by the uppermost occurrence of the *M. texana* zonal marker (Ogg, 2004b) (Figure 4).

Age and Occurrence: This biozone is delineated by the total range of *N. convexa* (Velić, 2007) and is attributed to the Late Albian (Ogg, 2004b). It occurs in marly limestones and limestones (28 m) of the Admir and Zbeideh sections. Here, the top of the biozone is determined by the FO of *Praealveolina iberica, Pseudolituonella reicheli, Nezzazata gyra* and *Nezzazata conica*. (Figures 3 and 4)

Praealveolina iberica interval zone (Ogg, 2004b), (*Conicorbitolina conica/ Conicorbitolina cuvillieri* range zone, Velić, 2007)

Diagnosis: Interval zone ranging from the FO of *Praealveolina iberica* to the FO of *Pseudedomia drorimensis.*

Description: The index fossils of Velić (2007) are not present in the studied section. We therefore introduced the *Praealveolina iberica* interval zone based on the FO of the marker species (compare Ogg, 2004b).

The *Praealveolina iberica* biozone is additionally characterized by the FO of the following three Cenomanian species: *P. iberica, Pseudolituonella reicheli* and *Charentia cuvillieri* that are associated with a rich assemblage of further Cenomanian benthonic foraminifera like *Trochospira avnimelechi, Nezzazata gyra, N. conica, Biconcava bentori, Moncharmontia apenninica, Pseudorhapydionina dubia, Merlingina cretacea, Vidalina radoicicae, Trocholina* sp. and *Gavelinella* sp.. They co-occur with some wide range species: *Ovalveolina crassa, Sellialveolina viallii, Cuneolina pavonia,* miliolids div. sp., *Nezzazata simplex, Nezzazatinella picardi, Pseudonummoloculina heimi, Nummoloculina* sp., *Peneroplis* sp., *Dictyopsella* sp.?, *Novalesia* cf. and *Marssonella* sp. (Figures 4 and 6d).

Correlation: The *Praealveolina iberica* interval zone is equivalent to the *Conicorbitolina conica/ Conicorbitolina cuvillieri* range zone (Velić, 2007), delineated by the range between the FO of *Praealveolina iberica* and the FO of *Pseudedomia drorimensis* (Ogg, 2004b) (Figure 4).

Age and Occurrence: The *P. iberica* interval zone represents the early Cenomanian and comprises the interval between the FO of *P. iberica, Pseudolituonella reicheli, Nezzazata gyra* and *Nezzazata conica* and the FO of *Pd. drorimensis, P. cretacea, P. brevis* and *P. tenuis* (Ogg, 2004b; Velić, 2007). In the South Palmyrides, this biozone represents early Cenomanian shallow marine limestones with high foraminiferal diversities (Figure 4). It occurs in unit 5 of the uppermost Zbeideh Formation, composed of (18 m) thick limestones in the Admir Section (Figure 7).

Pseudedomia drorimensis range zone (Ogg, 2004b)

Diagnosis: Total range zone of zonal marker.

Description: The *P. drorimensis* biozone is delineated by the total range of the zonal marker together with *Praealveolina tenuis* and *P. brevi*[illegible]riginally defined on the Adriatic Carbonate Platform (Velić, 2007). Several benthonic taxa were found that are well comparable with that biozone. Among those, *Sellialveolina* sp., *Hemicyclammina sigali, Nezzazatinella picardi, Praealveolina simplex, Pseudonummoloculina heimi, Pseudorhapydionina dubia, Nezzazata simplex, Nummoloculina regularis, Cuneolina pavonia* and miliolids div. sp. occur (Figures 4 and 6e).

Correlation: The *P. drorimensis* range zone according to the FO of the marker species (compare Ogg, 2004b). The latter author mentioned the co-occurrence with *Praealveolina iberica,* which, however, is restricted to the biozone below in the South Palmyrides (Figure 4).

Age and Occurrence: According to Ogg (2004b), the *P. drorimensis* biozone comprises the Middle to Upper Cenomanian (Figures 3 and 4). It is identified within a 45-m-thick succession of limestones, intercalated with marls and dolostones of the Abou-Zounnar Formation (Admir Section, Figure 7), equivalent to 75 m of marly limestones and limestones of the Zbeideh Section.

SEQUENCE STRATIGRAPHY

Within the integrated high-resolution stratigraphic framework of the latest Aptian to Late Cenomanian strata of the South Palmyrides, a sequence-stratigraphic model is here proposed. It is based on lithofacies characteristics, the geometric relationship of the strata, and their stacking pattern (i.e. the hierarchy of subcycles), microfacies interpretations, and stratigraphic attributions (Figures 7). Five depositional sequences, named South Palmyrides Sequence 1 to South Palmyrides Sequence 5, are here tentatively identified. Where possible the sequences are tied by biostratigraphic criteria to the maximum flooding surfaces (MFS) of Sharland et al. (2001, 2004) and sequences of Ogg (2004a).

South Palmyrides Sequence 1

In Syria a regional Lower Cretaceous unconformity separates the Jurassic Satih Formation from Lower Cretaceous basalt ([illegible]uty et al., 2003; Krasheninnikov et al., 2005). Intensive uplift, rifting, and volcanism correspond in the Palmyrides to the Tayasir basaltic volcanics of the Negev, Galilee High [illegible]gev and Rybakov, 2009) and Mount Lebanon area (Ferry et al., 2007). In the region of the Zbeideh Section, the volcanism was followed by the deposition of the Palmyra Formation in a fluvial setting, and then the Zbeideh Formation in a marginal-marine environment. South Palmyrides Sequence 1 consists of the Palmyra Formation and the lowermost Zbeideh Formation, which contains thin marly limestones with planktonic and benthonic foraminifera of latest Aptian age.

Early Albian MFS K90 (Sharland et al., 2004) was not confirmed in the South Palmyrides because of the absence of the *Hedbergella planispira* zone (Figures 4 and 7).

South Palmyrides Sequence 2 (around MFS K100)

The sequence boundary between sequences 1 and 2 is a hardground and unconformity/hiatus as evident by the missing *Hedbergella planispira* zone (Figures 4 and 7). South Palmyrides Sequence 2 represents the lower part of the Zbeideh Formation in the Zbeideh Section. It is composed of six shallowing-up subcycles (Figure 7). The basal two subcycles are nodular mudstones/wackestones with green algae, orbitolinids and planktonic foraminifera. The third subcycle consists of packstones with echinoderms, bivalves and gastropoda. The upper three subcycles are characterized by thinning-up stacking patterns from massive to laminated dolomite with chert nodules at the base (Figure 7).

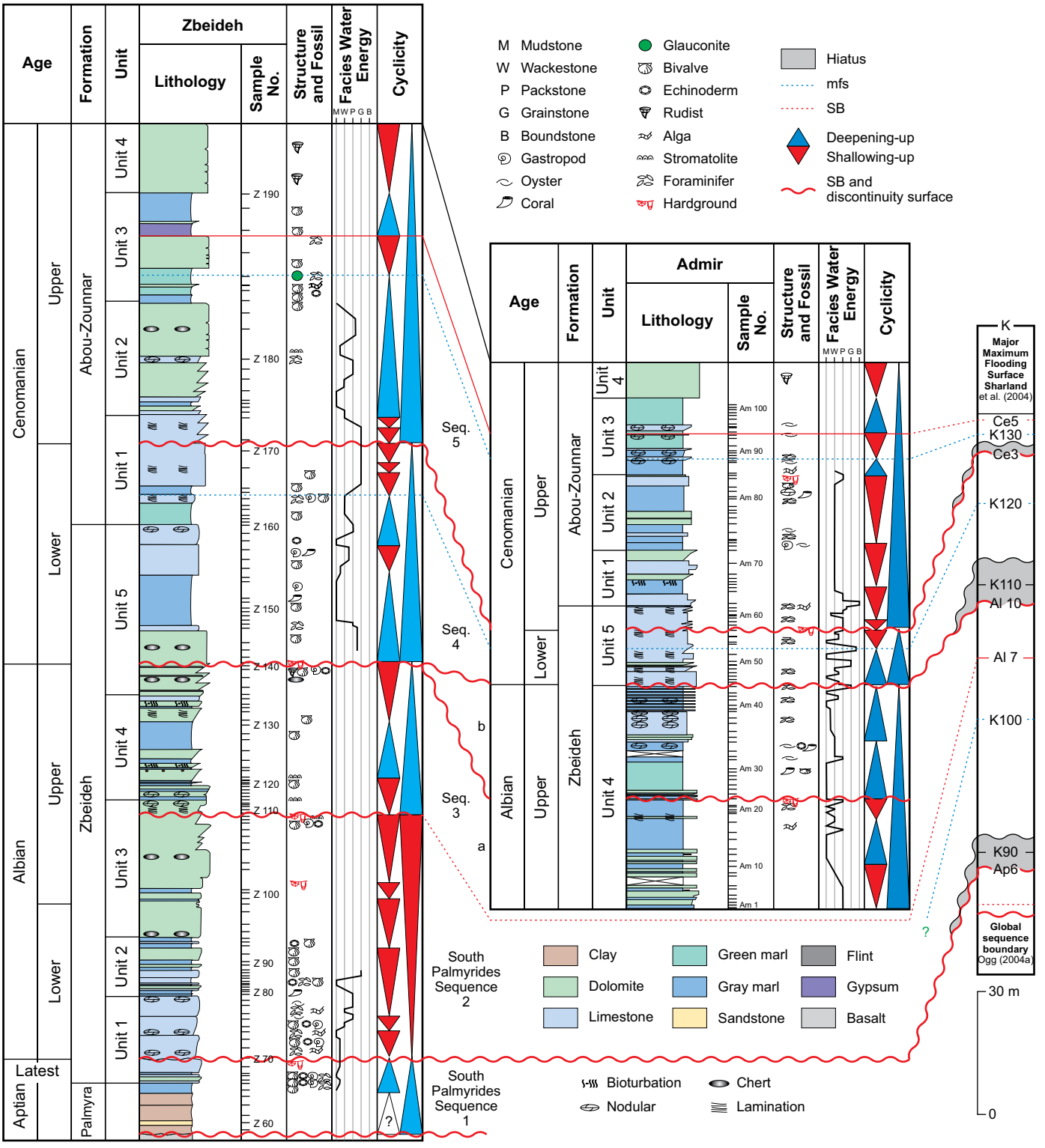

Figure 7: Correlation of the Palmyrides South sequences 1 to 5 in the Zbeideh and Admir sections South with the maximum flooding surfaces of the Arabia Plate (right column, after Sharland et al., 2001; Ogg, 2004a; Haq and Al-Qahtani, 2005).

Two shallow-water depositional settings are interpreted for the six shallowing-up subcycles of Sequence 2: the first three subcycles represent peritidal sediments, while the upper three subcycles are formed in shallow subtidal to supratidal environments.

The lower sequence boundary of Sequence 2 may correlate with the Late Aptian global sequence boundary SB AP6 of Ogg (2004a). A clear correlation of the Middle Albian MFS K100 of Sharland et al. (2004) with the shallow shelf limestones and dolomites of the Zbeideh Formation is hampered by their gross stratigraphic attribution within the *Mesorbitolina subconcava* zone.

South Palmyrides Sequence 3 (below MFS K110)

The sequence boundary between sequences 2 and 3 is a hardground within dolomites of the Zbeideh Formation of the Zbeideh Section. A similar hardground is missing in the Admir Section. However, the lower part of Sequence 3 is evidenced here by Upper Albian foraminifera (*Neoiraqia convexa*, *T. praeticinensis*). Therefore, we assume the lower boundary of Sequence 3 directly below the exposed part of the Admir Section (Figure 7).

The Upper Albian South Palmyrides Sequence 3 (divided into 3a and 3b) corresponds to the middle part of the Zbeideh Formation. It reflects a deepening-upwards cycle composed of three subcycles in both the Admir and Zbeideh sections (Figure 7). The basal subcycle shows a shallowing-up trend from restricted subtidal facies (bioclastic wackestone, peloidal pack-grainstone) to intertidal facies (laminated, stromatolites, dolo-mudstone). It is overlain by a deepening-up subcycle characterized by increasing diversity that reflects a local subcylic flooding surface on top of algal mound facies of the Admir Section. At the top of Sequence 3 a conspicuous fall of the sea level is evidenced by a hardground surface in both sections (Figure 7).

The middle part of the Zbeideh Formation of the Admir Section is composed of marly limestones with oysters, corals, echinoderms and of nodular limestones with planktonic foraminifera (Sequence 3b). Equivalent deposits are missing in the neighbouring Zbeideh Section. We therefore assume that the top of Sequence 3a (Zbeideh Section) was accompanied by erosion and/or amalgamation of synchronous Admir deposits of Sequence 3b (Figure 7).

The Upper Albian global sequence boundary Al7 of Ogg (2004a) is comparable to the lower boundary of Sequence 3. The Late Albian MFS K110 (Sharland et al., 2004) could not be identified in the South Palmyrides because of a major hiatus that spans the *Rotalipora appenninica* zone (Figures 4 and 7).

South Palmyrides Sequence 4 (including MFS K120)

Sequence 4 corresponds to the uppermost Zbeideh Formation and the lowermost Abou-Zounnar Formation in the Zbeideh Section, and to the uppermost Zbeideh Formation of the Admir Section. The base of the Lower Cenomanian South Palmyrides Sequence 4 coincides with the Albian/ Cenomanian hiatus (Figure 4). It may correlate with the Late Albian SB Al10 of Ogg (2004a) (Figure 7). The sequence is composed of two deepening-upwards subcycles overlain by three shallowing-upwards subcycles in the Zbeideh Section. In the Admir Section, the sequence consists of only one deepening-upwards and one shallowing-upwards subcycle (Figure 7).

The deepening-upwards subcycles of both sections are composed of well-bedded to laminated, fine-grained limestones (wackestone to packstone, rich in heavily micritized large benthonic foraminifera), serpulids and large bivalves. The overlying shallowing-upwards subcycle(s) contain mainly wackestones with trocholinids and boundstones (red algae). In addition, bioturbated mudstones and wackestones occur, with shallow water benthonic foraminifera (praealveolinids, *Cuneolina*, nezazzatids), rare gastropods and bivalves.

The deepening-upwards cycle(s) are interpreted to represent mainly open-marine shallow subtidal environments, the shallowing-upwards cycle(s) are attributed to open lagoonal environments. The lower number of subcycles in the Admir Section is possibly due to lower sedimentation rates.

The Lower Cenomanian MFS K120 of Sharland et al. (2004) corresponds to laminated fossiliferous limestones of the upper *R. globotruncanoides* zone of the Admir Section (Figures 4 and 7). A correlation with laminated limestones of the Zbeideh Section is mainly based on comparisons of the stacking patterns.

South Palmyrides Sequence 5 (including MFS K130)

The lower boundary of the Upper Cenomanian South Palmyrides Sequence 5 in the Admir Section is represented by a hardground surface (Figure 9), associated with a hiatus spanning the *Rotalipora reicheli* zone. This boundary is comparable to the Middle Cenomanian SB Ce3 of Ogg (2004a).

Sequence 5 corresponds to the uppermost Zbeideh to Abou-Zounnar formations of the Admir Section, and to the Abou-Zounnar Formation in the Zbeideh Section. Sequence 5 is composed of thin to massive nodular white dolomites and limestones with few corals, bivalves, gastropods and ostracods. Green and gray marls above with abundant oysters and intercalated thin pelagic limestones are overlain by gypsum-rich marls in the Zbeideh Section. Massive dolomites (unit 4) of both sections contain disarticulated, complete or dissolved rudists (dolomitized bioturbated float- to wackestones) (Figure 7).

The general deepening-upwards trend of both the Zbeideh and Admir sections exhibits subcyclic stacking patterns (Figure 7): four shallowing-upwards subcycles in the Admir Section correspond to two minor shallowing-upwards subcycles in the Zbeideh Section. Synchronous stacking patterns of two deepening-upwards and two shallowing-upwards subcycles follow above in both sections.

The rapid increase of planktonic foraminifera and glauconite of unit 3 of both sections (*Pseudedomia drorimensis* and *Rotalipora cushmani* biozones) corresponds to MFS K130 (Sharland et al., 2004; Haq and Al-Qahtani, 2005). It coincides in both sections with the boundary between a shallowing-upwards and a deepening-upwards subcycle (Figure 7). The evaporitic marly interval above (unit 3 of Zbeideh Section) may correspond with the uppermost Cenomanian SB Ce5 of Ogg (2004a), which is represented by another subcyclic boundary in both the Zbeideh and Admir sections (Figure 7).

CARBON ISOTOPES

Carbon-isotope records of shallow-water limestones are sensitive to early diagenetic alteration due to subaerial exposure of the seafloor (Joachimski, 1994) and to burial diagenesis. Moreover, the $\delta^{13}C$ ratios may be influenced by isotopically light carbon from soil zone CO_2 (Allan and Matthews, 1982). Our microfacies interpretations of pure limestones and marls indicate that most isotope data are not influenced by syn-sedimentary soil zone or karstic processes. However, the interaction with diagenetic fluids may have converted the original stable-isotope signature of marine carbonates (compare Parente et al., 2007), as indicated by diagenetic processes of the mixing-zone in both intervals D_1 and D_2 of the Admir Section (Figure 11). Consequently we excluded ten samples of the D_1-interval (negative $\delta^{13}C$ values) and 10 samples of the D_2-interval (wide fluctuations of $\delta^{18}O$ values coinciding with dolomitic intercalations) for further considerations. The adjusted curve (Figure 11b) was used for the comparison of the Late Albian–Late Cenomanian isotopic record of the Palmyrides with age-equivalent strata (Luciani et al., 2006; Kennedy et al., 2004; Jarvis et al., 2006) (Figures 8, 10 and 12).

Major Trends of the Carbon-isotope Signature

The carbon-isotope variations of the studied Late Albian–Late Cenomanian interval of the Admir Section (Figures 8 and 10) allows for the biostratigraphic comparison and calibration of the planktonic and benthonic foraminifera biozonation, and the determination of organic-matter-rich intervals that are correlated with oceanic anoxic events (OAEs). Based on our sequence-stratigraphic interpretations, the $\delta^{13}C$ curve was split into three segments South Palmyrides sequences 3, 4, 5, separated by hiatuses (Figure 10), and compared with age-equivalent $\delta^{13}C$ records documented by Luciani et al. (2006), Kennedy et al. (2004) and Jarvis et al. (2006).

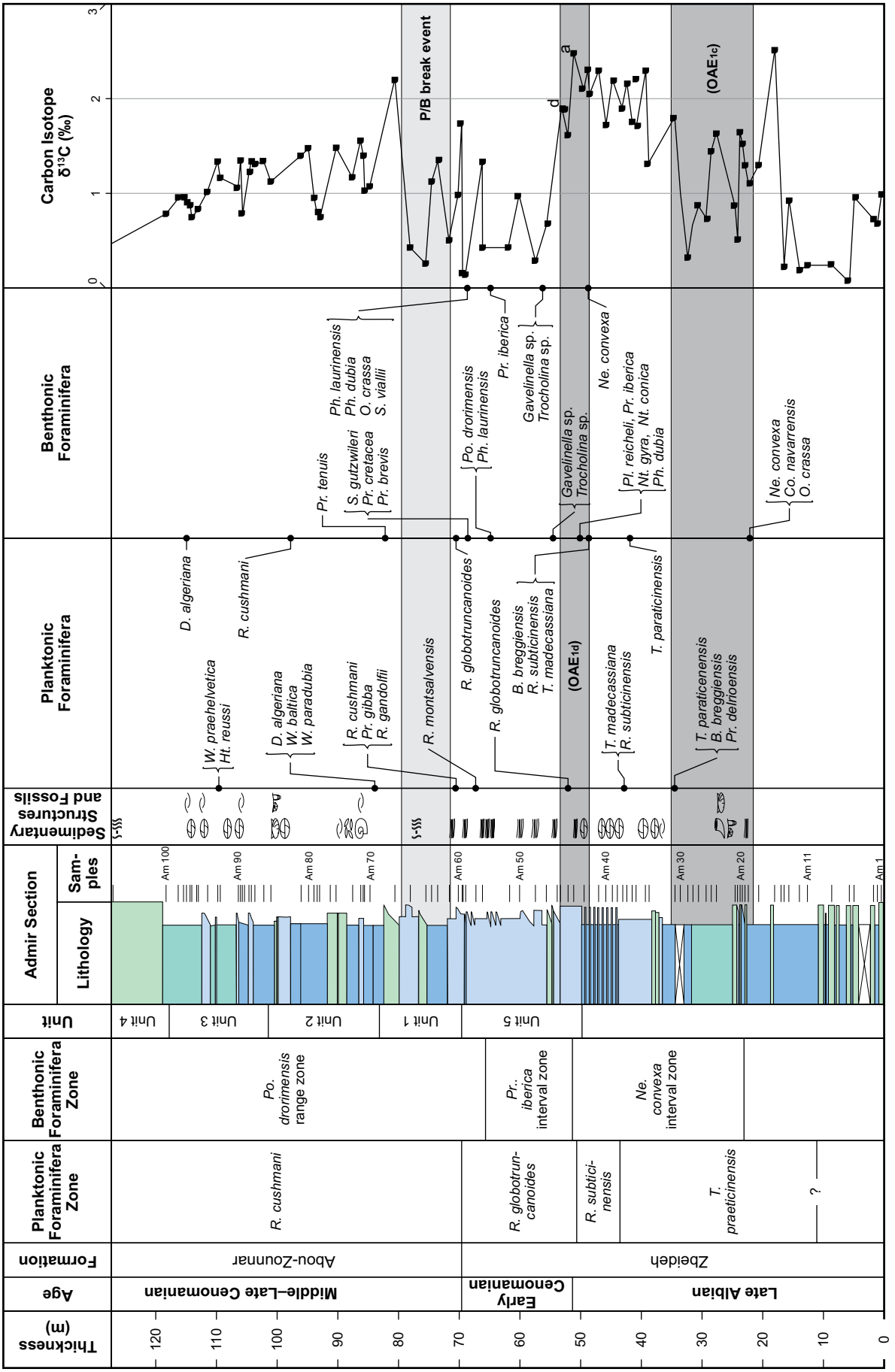

Figure 8: Biostratigraphy of the Admir Section compared with $\delta^{13}C$ fluctuations (stippled line indicates third average values). Several $\delta^{13}C$ events allow for comparison with those defined by Friedrich (2010), Jarvis et al. (2006), Luciani et al. (2006), and Kennedy et al. (2004). Compare to Figure 10 for a detailed correlation around the Albian/Cenomanian boundary. For lithological colors see Figure 7.

Figure 9: Hardground surface with vertical burrows indicates the Lower Cenomanian discontinuity surface Ce3 (section Admir, Figure 7).

The early Late Albian record of the Admir Section starts with positive $\delta^{13}C$ values and reaches a short maximum of 2.9‰. The following $\delta^{13}C$ values of an overlying 12-m-thick unit (Figure 10) are well comparable to the age-equivalent OAE1c-interval of the $\delta^{13}C$-curve of Coppa della Nuvola (Luiciani et al., 2006). The similar trend of both early Late Albian curves is evident (Figure 10).

During the latest Albian, carbon-isotope values increased and reached nearly constant values of ca. 2.6‰ at the Admir Section. A short decline of $\delta^{13}C$ values directly above the LO of *R. subticinensis* was compared with the Breistroffer-Event of the Mount Risou Section (Kennedy at al., 2004), corresponding to peak a (Figure 10). The Albian/Cenomanian boundary at Mount Risou spans a broad positive excursion (subdivided into four discrete peaks a to d). Comparable strata are nearly completely missing at the Admir Section, due to a major hiatus. Here, the Lower Cenomanian strata record $\delta^{13}C$ values that may correlate with peak d of Kennedy et al. (2004), confirmed by *R. globotruncanoides* (Figure 5). The overlying sediments of South Palmyrides Sequence 4 correlate with a thin Lower Cenomanian interval that is topped by a thin positive excursion of $\delta^{13}C$-values, probably equivalent to LCE I of Jarvis et al. (2006) (Figure 10).

Following a major hiatus (*R. reicheli* biozone) the third segment of the $\delta^{13}C$ curve of the Admir Section spans a Middle to Upper Cenomanian interval (South Palmyrides Sequence 5 – Figure 10). Compared to Jarvis et al. (2006), the $\delta^{13}C$-values of the Palmyrides show several discrepancies, probably due to diagenetic overprint (Figure 10).

Oceanic Anoxic Event 1c, Albian/Cenomanian Boundary and Planktonic/Benthonic Break Event

The $\delta^{13}C$ curve of the Admir Section was calibrated with biostratigraphic results (based on benthonic and planktonic foraminifera) of the Late Albian to Late Cenomanian succession. Significant perturbations of the foraminiferal diversity, abundance or their total absence are compared with $\delta^{13}C$-values to highlight the Late Abian to Late Cenomanian biotic events and possible equivalents of Oceanic Anoxic Events (OAE) (Jarvis et al., 1988, 2006; Luiciani et al., 2004, 2006; Friedrich, 2010).

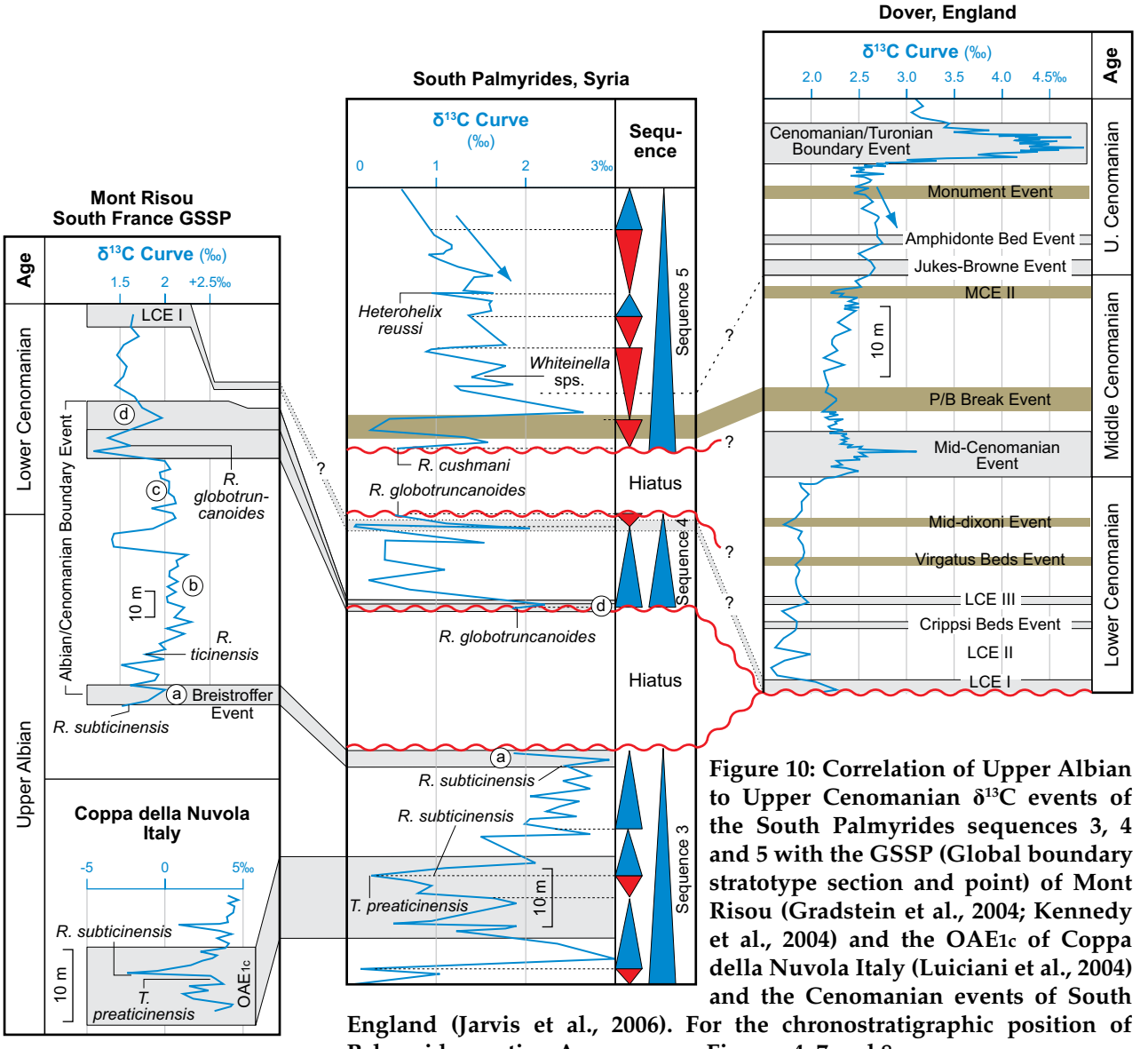

Figure 10: Correlation of Upper Albian to Upper Cenomanian $\delta^{13}C$ events of the South Palmyrides sequences 3, 4 and 5 with the GSSP (Global boundary stratotype section and point) of Mont Risou (Gradstein et al., 2004; Kennedy et al., 2004) and the OAE1c of Coppa della Nuvola Italy (Luiciani et al., 2004) and the Cenomanian events of South England (Jarvis et al., 2006). For the chronostratigraphic position of Palmyrides section Am, compare Figures 4, 7 and 8.

OAE1c Event

The lower Upper Albian $\delta^{13}C$ values of the Admir Section are generally comparable to those of the Nuvola in Italy (Luiciani et al., 2004, 2006). The lower Upper Albian $\delta^{13}C$ values of South Italy fall to -2.6‰ and rise to values between 0.8‰ to 2‰ in the upper *T. praeticinensis* to the lowermost *R. subticinensis* zones (Luiciani et al., 2006). In the Admir Section the $\delta^{13}C$ values remain within the range 0.1‰ to 2.3‰ in the same biostratigraphic interval. The OAE1c Event is marked by the LO of *T. praeticinensis* and the FO of *R. subticinensis*, and the associated planktonic foraminifera of this biozone (Figures 10).

Albian/Cenomanian Boundary Event (Wilson and Norris, 2001; Kennedy et al., 2004; Friedrich, 2010)

Although most parts of the Albian/Cenomanian Boundary Event are missing in the South Palmyrides (hiatus), its lower boundary (Peak a: Breistroffer event, Figure 10) and its upper boundary (Peak d, Figure 10) are biostratigraphically confirmed. Therefore it is possible to discuss the correlation of carbon-isotope values.

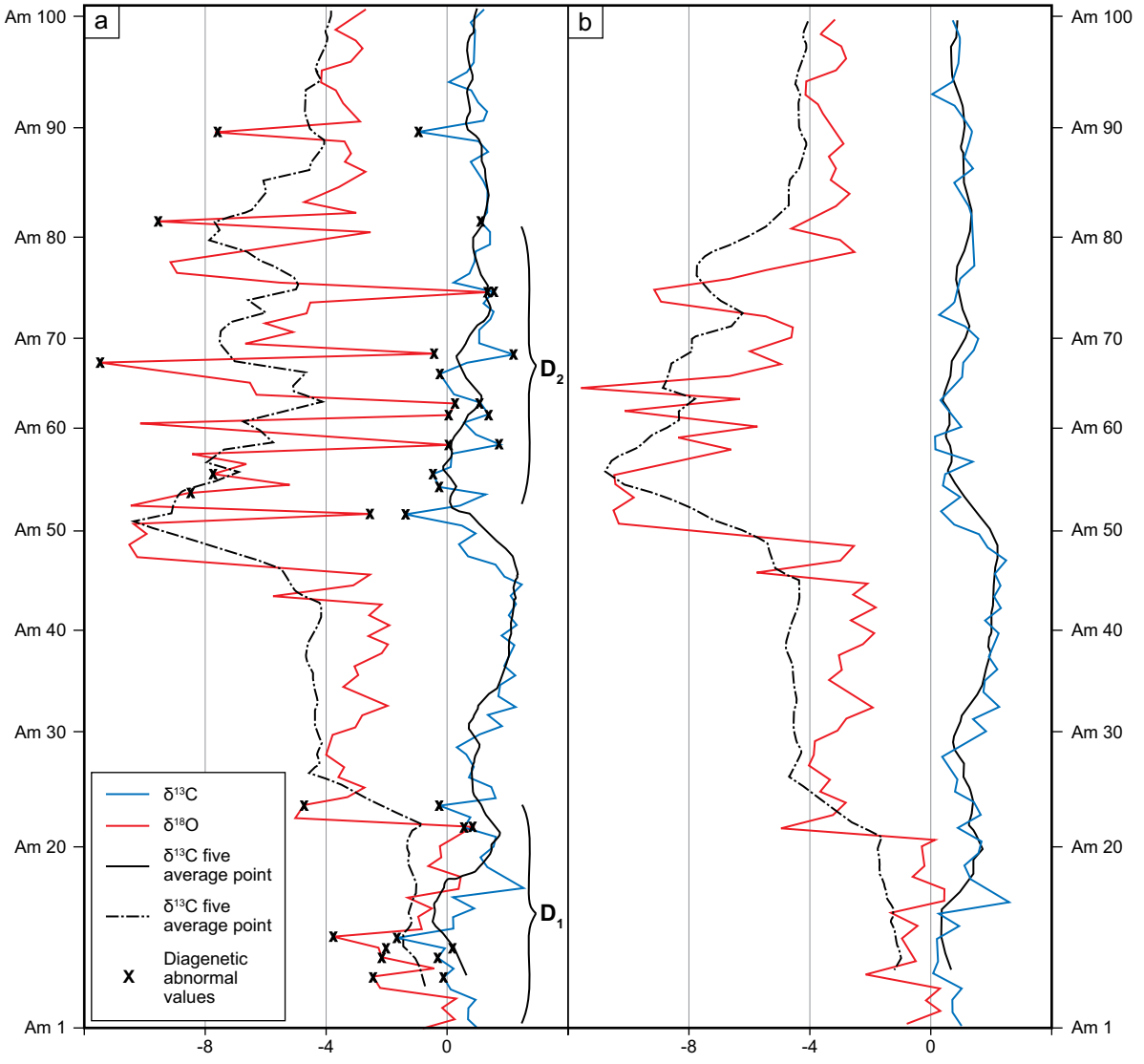

Figure 11: Stable-isotope curves ($\delta^{18}O$, $\delta^{13}C$) of the Admir Section. Samples Am-1 to Am-101 refer to Figure 7.

(a) Measured $\delta^{18}O$ between (1‰ and -10‰) and $\delta^{13}C$ (between ca. 3‰ and -2.7‰). D1 and D2 correspond to meteoric and subaerial diagenetic intervals.

(b) $\delta^{18}O$ and $\delta^{13}C$ curves after excluding 10 high negative $\delta^{13}C$ values and 10 extreme widely fluctuating $\delta^{18}O$ values, marked with X in (a). The curve $\delta^{13}C$ of (b) was used in Figures 5 and 10.

The carbon-isotope curve shows maximum values of 2.3‰ to 2.7‰ within a 5-m-thick interval near the Albian/Cenomanian boundary (Admir Section, Figures 5 and 10). These values demonstrate two peaks (lettered a and d, Figure 10) that occur within marly limestones intercalating with nodular limestones (Peak a), unconformably overlain by massive limestones (Peak d) of the Admir Section (Figures 5 and 10). Peaks a and d are comparable with two of the four minor peaks (a to d) defined around the Albian/Cenomanian boundary of Mont Risou (GSSP section; Kennedy et al., 2004, compare Figure 10). The correlation between the South Palmyrides $\delta^{13}C$ curve and that from Mont Risou (with respect to the Albian/Cenomanian boundary, Figure 10) is based on our new biostratigraphic data around the Late Albian hiatus (Figure 3) combined with the new $\delta^{13}C$ variations of the Admir Section. The following arguments favor the correlation: Peak d coincides with the first event (Breistroffer event), determined by the LO of *R. subticinensis*. In the Admir Section, however, a gap is registered between LO of *R. subticinensis* and the FO of *R. globotruncanoides*

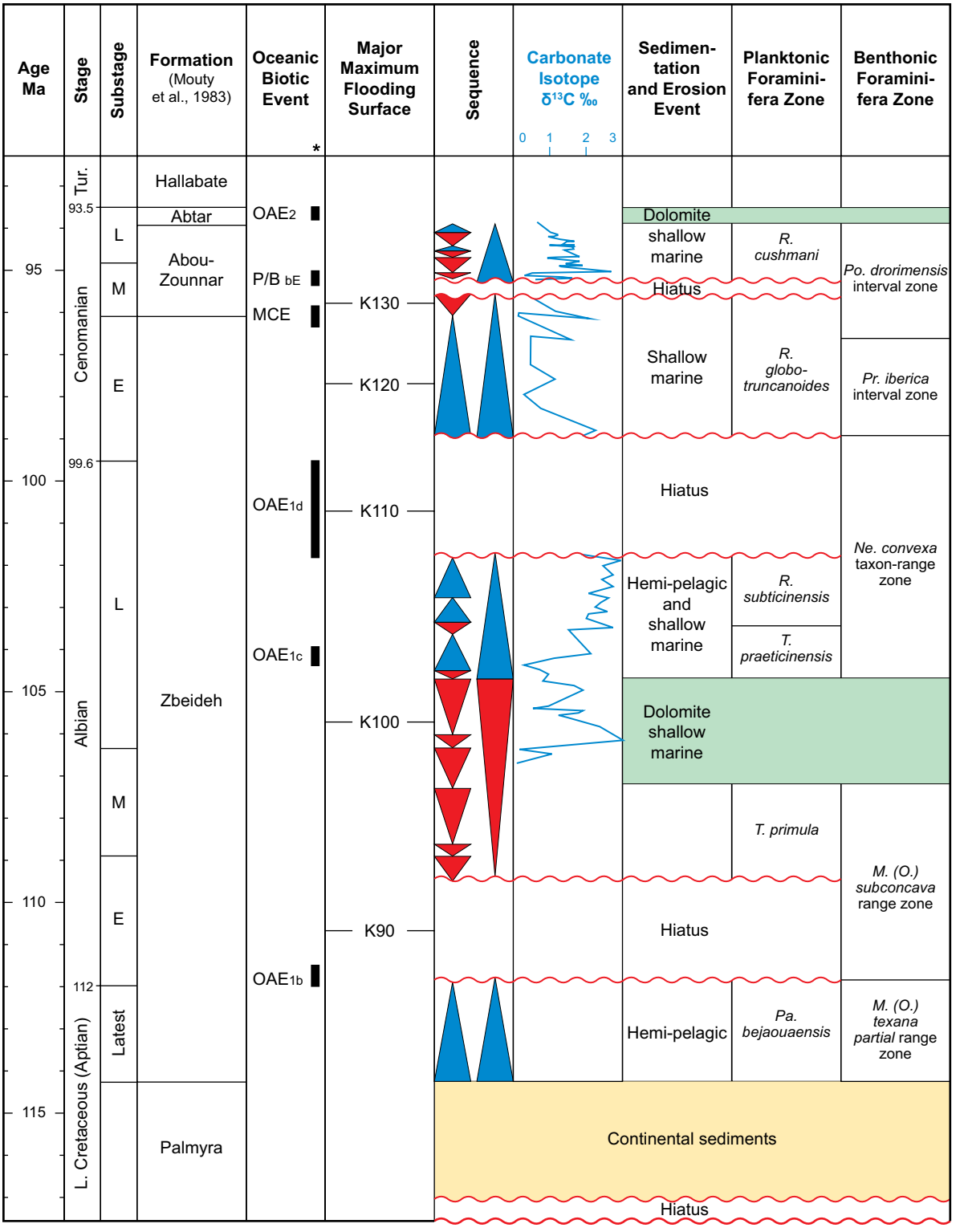

Figure 12: Summary of major stratigraphic events, including sequence-stratigraphic interpretation, of the Lower to middle Cretaceous succession in the South Palmyrides. * = Friedrich, 2010; Jarvis et al., 2006; Lucia et al., 2004.

(based on the missing of both biozones *R. ticinensis* and *R. appenninica*), equivalent to the postulated hiatus in the South Palmyrides carbonate platform.

Planktonic/Benthonic (P/B) Break Event

This event is explained by a dramatic increase of both diversity and abundance of the planktonic foraminifera (see description of the *Rotalipora cushmani* zone above; Figures 3 and 5). The $\delta^{13}C$ signature of this bio-event is represented by falling $\delta^{13}C$ values (0.3‰), contrasting to a slight increase recorded by Jarvis et al. (2006; Figures 5 and 10). At this level the abundance of the planktonic foraminifera has been used as a marker; moreover, this interval is characterized by the FO of *R. cushmani* (compare Jarvis et al., 2006).

The characteristic of Upper Cenomanian $\delta^{13}C_{carb}$

The Upper Cenomanian $\delta^{13}C$ curve of the Admir Section ranges between 1.2‰ and 1.5‰. The correlation with Jarvis et al. (2006) suggests that the base of the Upper Cenomanian of the South Palmyrides is defined very close to the FO of the genus *Whiteinella.* In addition, the Amphidonte Bed Event is stratigraphically comparable with the FO of *Heterohelix reussi* (Ogg, 2004a) (Figure 10). The carbon-isotope excursion of the Tethys realm of Jarvis et al. (2006) and the South Palmyrides has similar decreasing of $\delta^{13}C$ above the Amphidonte Bed Event (Ogg, 2004a; Jarvis et al., 2006) (Figure 10).

CONCLUSIONS

Detailed stratigraphic studies on limestones were conducted in two sections from the shallow carbonate platform of the South Palmyrides, Syria. They allowed us to reconstruct the uppermost Aptian to Upper Cenomanian framework, based on planktonic foraminiferal biostratigraphy (Ogg, 2004a, b; Premoli Silva and Verga, 2004), benthonic foraminiferal biostratigraphy (Velić, 2007; Schroeder et al., 2010), and $\delta^{13}C$ fluctuations (Kennedy et al., 2004; Jarvis et al., 2006). New biostratigraphic data was used to correlate global biotic and abiotic events with local events of the South Palmyrides: OAE1c, Albian/Cenomanian boundary, and Planktonic/Benthonic break.

Missing planktonic and benthonic biozones and thick dolomitic intervals were used to define four major stratigraphic hiatuses: The Early Albian hiatus of the *Mucrohedbergella planispria* biozone; the Late/Middle Albian dolomitic hiatus, the Late Albian/Early Cenomanian hiatus spanning the *Rotalipora ticinensis* and *R. appenninca* biozones, and the Mid Cenomanian hiatus of the *Rotalipora reicheli* biozone.

With the recovery of hemipelagic conditions in the South Palmyrides Basin during latest Aptian, the continuous marine succession (latest Aptian to Late Cenomanian) reflects two main episodes of maximum sea-level rise comparable with the maximum flooding surfaces MFS K120 and MFS K130 of the Arabian Plate (Sharland et al., 2004). Major hiatuses and hardgrounds were interpreted as sequence boundaries of five local sequences, South Palmyrides sequences 1 to 5, which stratigraphically correspond with some of the third-order global sequences of Ogg (2004a).

ACKNOWLEDGEMENTS

We are indebted to Ahmed A.M. Abd El-Naby, Geology Department, Ain Shams University (Egypt) for his help and Christian Scheibner, Geochronology Department, Bremen University (Germany) for his support. We would like to extend our special thanks to our colleagues of the Geochronology working group in Bremen University for various help. We thank GeoArabia's three anonymous reviewers for their helpful comments, Arnold Egdane for designing the paper for press, and Kathy Breining for proof-reading it.

REFERENCES

Allan, J.R. and R.K. Matthews 1982. Isotope signatures associated with early meteoric diagenesis. Sedimentology, v. 29, p. 797-817.

Al-Maleh, A.KH. M. Mouty, T. Sawaf, G. Brew and M. Barazangi 2000. Mesozoic depositional trends in the northern Arabian Platform in Syria; regional and tectonic implications. GeoArabia, v. 5, no. 1, p. 30-31.

Boudagher-Fadel, M.K. 2008. Evolution and Geological Significant of Lager Benthic Foraminifera, Developments in Paleontology and Stratigraphy. Elsevier, Amsterdam, 544 p.

Caron, M. 1985. Cretaceous planktic foraminifera. In H.M. Bolli, J.B. Saunders and K. Perch-Nielsen (Eds.), Plankton Stratigraphy. Cambridge University Press, p. 17-86.

Ferry, S., Y. Merran, D. Grosheny and M. Mroueh 2007. The Cretaceous of Lebanon in the Middle East (Levant) context [*Le Crétacé du Liban dans le cadre du Moyen-Orient (Levant)*]. Carnets de Géologie, p. 38-42.

Friedrich, O. 2010. Benthic foraminifera and their role to decipher paleoenvironment during mid-Cretaceous Oceanic Anoxic Events – the "anoxic benthic foraminifera" paradox. Revue de Micropaleontologie, v. 53, p. 175-192.

Gale, A.S., W.J. Kennedy, J.A. Burett, M. Caron and B.E. Kidd 1996. The Late Albian to Early Cenomanian succession at Mont Risou near Rosans (Drome, SE France): An integrated study (ammonites, inoceramids, planktonic foraminifera, nannofossils, oxygen and carbon isotopes). Cretaceous Research, v. 17, p. 515-606.

Gradstein, F.M., J.G. Ogg and A.G. Smith 2004. A Geologic Time Scale 2004. Cambridge University Press, 589 p.

Haq, B.U. and A.M. Al-Qahtani 2005. Phanerozoic cycles of sea-level change on the Arabian Platform. GeoArabia, v. 10, no. 2, p.127-160.

Homberg, C. and M. Bachmann 2010. Evolution of the Levant margin and western Arabian Platform since the Mesozoic: Introduction. Geological Society, London, v. 341, p. 1-8.

Jarvis, I., G.A. Carson, M.K. Cooper, M.B. Hart, P.N. Leary, B.A. Tocher, D. Horne and A. Rosenfeld 1988. Microfossil assemblages and the Cenomanian-Turonian (late Cretaceous) oceanic anoxic event. Cretaceous Research, v. 9, p. 3-103.

Jarvis, I., A.S. Gale, H.C. Jenkyns and M.A. Pearce 2006. Secular variation in Late Cretaceous carbon isotopes: A new $\delta^{13}C$ carbonate reference curve for the Cenomanian–Campanian (99.6–70.6 Ma). Geological Magazine, v. 143, p. 561-608.

Joachimski, M.M. 1994. Subaerial exposure and deposition of shallowing upward sequences: Evidence from stable isotopes of Purbeckian peritidal carbonates (basal Cretaceous), Swiss and French Jura Mountains. Sedimentology, v. 41, p. 805-824.

Kennedy, W.J., A.S. Gale, J.A. Lees and M. Caron 2004. The global boundary stratotype section and point (GSSP) for the base of the Cenomanian Stage, Mont Risou, Hautes-Alpes, France. Episodes, v. 27, no.1, p. 21-32.

Krasheninnikov, V.A., J.K. Hall, F. Hirsch, C. Benjamini and A. Flexer (Eds.) 2005. Geological framework of the Levant, Volume I: Cyprus and Syria, p. 165-416.

Kuss, J., A. Bassiouni, J. Bauer, M. Bachmann, A. Marzouk, C. Scheibner and F. Schulze 2003. Cretaceous – Paleogene Sequence Stratigraphy of the Levant Platform (Egypt, Sinai, Jordan). In E. Gili, H. Negra and P. Skelton (Eds.), North African Cretaceous Carbonate Platform Systems. Nato Science Series, p. 171-187.

Loeblich, A.R. and H. Tappan 1988. Foraminiferal genera and their classification. Van Nostrand Reinhold Co., New York, 970 p.

Luiciani, V., M. Cobianchi and H.C. Jenkyns 2004. Albian high-resolution biostratigraphy and isotope stratigraphy: The Coppa della Nuvola pelagic succession of the Gargano Promontory (Southern Italy). Eclogae Geologicae Helvetiaev, 97, p. 77-92.

Luiciani, V., M. Cobianchi and C. Lupi 2006. Regional record of a global oceanic anoxic event: OAE1a on the Apulia Platform margin, Gargano Promontory, southern Italy. Cretaceous research, v. 27, p. 754-772.

Mouty, M. 1997. Le Jurassique de la chaîne des Palmyrides, Syrie centrale. Bulletin of the French Geological Society, France, v. 168, p. 181-186.

Mouty, M., A.KH. Al-Maleh, H. Abou-Laban and Y. Al-Joubeli 1983. The geological study of the Palmyridean chain through typical geological sections. The General Establishment of Geology and Mineral Resources. C No. 140/NA.

Mouty, M., A.KH. Al-Maleh and H. Abou-Laban 2003. Le Crétacé moyen la chaîne des Palmyrides (Syrie centrale). Geodiversitas, Paris, v. 25, p. 429-443.

Ogg, J.G. 2004a. Mid- Late Cretaceous Charts. http://norges.uio.no/timescale/Late_Cretaceous.pdf and, http://norges.uio.no/timescale/Early_Cretaceous.pdf.

Ogg, J.G. 2004b. Mid- Late Cretaceous Charts. In F.M. Gradstein, J.G. Ogg and A.G. Smith (Eds.), A Geologic Time Scale 2004. Cambridge University Press, 589 p.

Parente, M., G. Frijia and M. Dilucia 2007. Carbon-isotope stratigraphy of Cenomanian–Turonian platform carbonates from the southern Apennines (Italy): A chemostratigraphic approach to the problem of correlation between shallow-water and deep-water successions. Journal of the Geological Society, London, v. 164, p. 609-620.

Ponikarov, V.P., V.G. Kazmin, I.A. Mikhailov, A.V. Razvaliayev, V.A. Krasheninnikov, V.V. Kozlov, E.D. Soulidi-Kondtatiyev and V.A. Faradzhev 1966. The Geological map of Syria. 1:1,000,000. Explanatory Notes. Technoexport, USSR, 111 p.

Premoli Silva, I. and D. Verga 2004. Practical manual of Cretaceous planktonic foraminifera. In D. Verga, R. Rettori (Eds.), International School on Planktonic Foraminifera: Perugia, Italy, Tipografia Ponte Felcino, Universities of Perugia and Milan, 3rd Course, 283 p.

Premoli Silva, I., M. Le Caron, R.M. Leckie, M.R. Petrizzo, D. Soldan and D. Verga 2009. Paraticinella Gen and Taxonomic Revision of *Ticinella Bejaouaensis* Sigal 1966. Journal of Foraminiferal Research, v. 39, no. 2, p.126-137.

Schroeder, R. and M. Neumann 1985. Les grands foraminifères du Crétacé moyen de la région Méditerranéenne. Geobios, Mémoire Spécial 7, p. 1-160.

Schroeder, R., F.S.P. van Buchem, A. Cherchi, D. Baghbani, B. Vincent, A. Immenhauser and B. Granier 2010. Revised orbitolinid biostratigraphic zonation for the Barremian – Aptian of the eastern Arabian Plate and implications for regional stratigraphic correlations. In F.S.P. van Buchem, M.I. Al-Husseini, F. Maurer and H.J. Droste. Barremian – Aptian Stratigraphy and Hydrocarbon Habitat of the Eastern Arabian Plate. GeoArabia Special Publication 4, Gulf PetroLink, Bahrain, v. 1, p. 49-96.

Sharland, P.R., R. Archer D.M. Casey, R.B. Davies, S.H. Hall, A.P. Heward, A.D. Horbury and M.D. Simmons 2001. Arabian Plate sequence stratigraphy. GeoArabia Special Publication 2, Gulf PetroLink, Bahrain, 371 p., with 3 charts.

Sharland, P.R., D.M. Casey, R.B. Davies, M.D. Simmons and O.E. Sutcliffe 2004. Arabian Plate Sequence Stratigraphy. GeoArabia, v. 9, no. 1, p. 199-214**.**

Sigal, J. 1966. Contribution a` une monographie des Rosalines. 1. Le genre *Ticinella Reichel*, souche des Rotalipores. Eclogae Geologicae Helvetiae, v. 59, p. 186-217.

Stampfli, G.M., J. Mosar, P. Favre, A. Pillevuit and J.-C. Vannay 2001. Permo-Mesozoic evolution of the western Tethyan realm: The Neotethys/East-Mediterranean connection. In P.A. Ziegler, W. Cavazza, A.H.F. Robertson and S. Crasquin-Soleau (Eds.), Peritethys, Memoir 6: Peritethyan Rift/ Wrench Basins and Passive Margins, IGCP 369. Memorial Museum of Natural History, v. 186, p. 51-108.

Velić, I. 2007. Stratigraphy and palaeobiogeography of Mesozoic benthic foraminifera of the karst dinarides (SE Europe). Geologia Croatica, v. 60, no. 1, p. 1-113.

Wilson, P.A. and R.D. Norris 2001. Warm tropical ocean surface and global anoxic during the mid-Cretaceous period. Nature, v. 412, p. 425-429.

ABOUT THE AUTHORS

Hussam Ghanem *is currently working towards his PhD in Geochronology at Bremen University. His research is focused on stratigraphy evolution of carbonate platform (Cretaceous of Syria) and the interpretation of Syrian tectonic history through Sedimentary analysis. He obtained a MSc in Geology and worked for a short time with Petro- service Syria.*

hussam_ghanem@yahoo.com

Mikhail Mouty *is President of Geological Consulting Group, Syria. Prior to that he was a Professor in the Department of Geology at Damascus University, Syria. Mikhail has been Head of the Geology Department with the Syrian Atomic Energy Commission, and Head of Geological Society of Syria. He has "Licence es Sciences Naturelles" from Damascus University and "Doctorat es Sciences Geologiques et Minéralogiques" from Geneva University, Switzerland. His research includes Mesozoic stratigraphy in Syria and the Middle East.*

mouty@scs-net.org

Jochen Kuss *was awarded a PhD in 1983 by Erlangen University in Germany following studies on Upper Triassic ramp deposits in the northern Calcareous Alps. From 1983 to 1991 he was an Assistant Professor at the Technical University of Berlin and undertook sedimentologic and stratigraphic work in Egypt and Jordan. In 1991 Jochen joined the University of Bremen. His main research interests are field work-based studies of marine Cretaceous to Paleogene successions in North Africa and the Middle East. Methods used include petrography, (micro) biostratigraphy, geochemistry, remote sensing and basin modeling.*

kuss@uni-bremen.de

Manuscript received February 28, 2011;

Revised July 28, 2011;

Accepted August 12, 2011